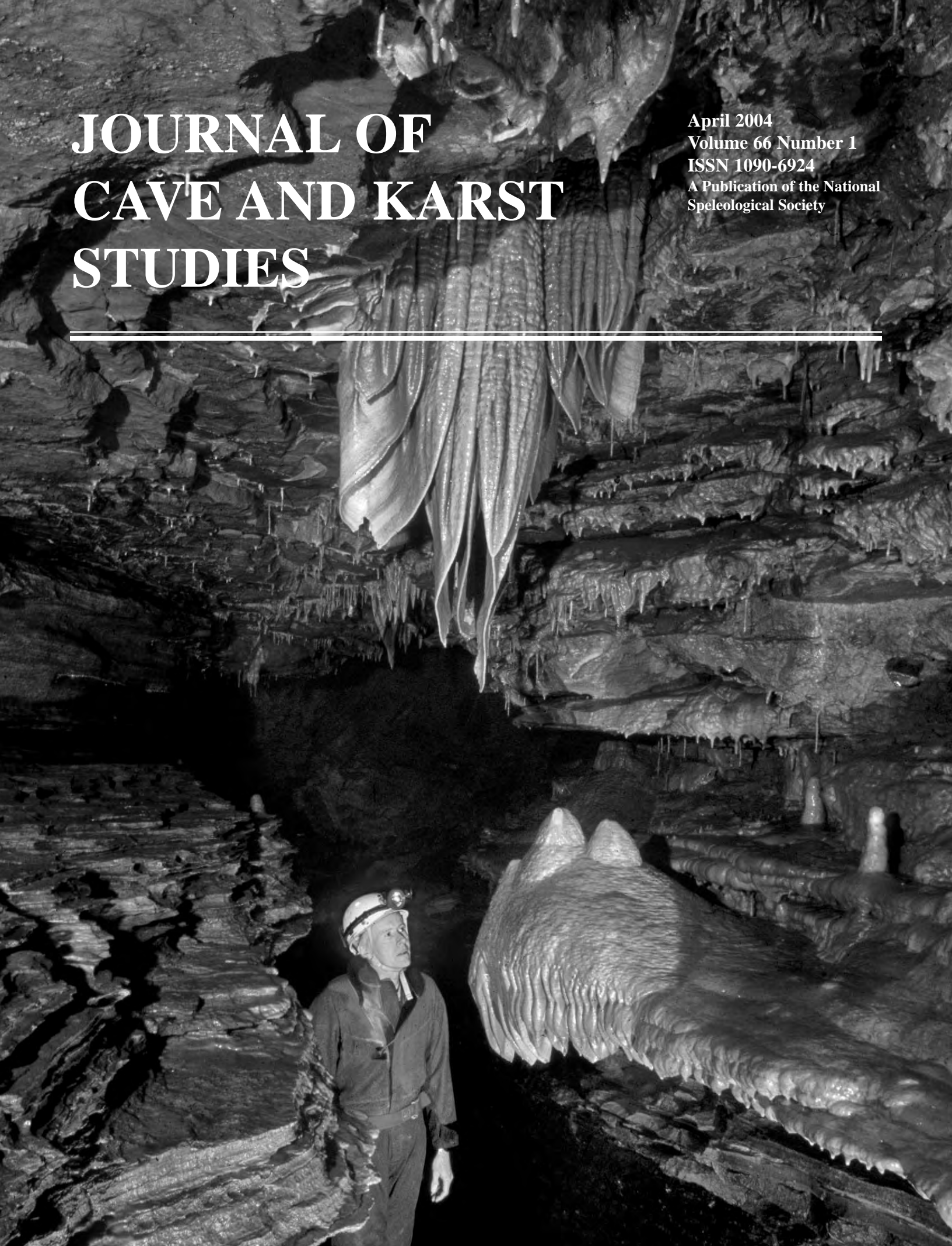


JOURNAL OF CAVE AND KARST STUDIES

April 2004
Volume 66 Number 1
ISSN 1090-6924
A Publication of the National
Speleological Society



Journal of Cave and Karst Studies of the National Speleological Society

Volume 66 Number 1 April 2004

CONTENTS

Editorial

Malcolm S. Field 3

Article

Application of high-resolution X-ray computed tomography in determining the suitability of speleothems for use in paleoclimatic, paleohydrologic reconstructions
Patrick J. Mickler, Richard A. Ketcham, Matthew W. Colbert, and Jay L. Banner 4

Comparison of a new GIS-based technique and a manual method for determining sinkhole density:
An example from Illinois' sinkhole plain
Julie C. Angel, Daniel O. Nelson, and Samuel V. Panno 9

Stygobites are more wide-ranging than troglobites
John Lamoreux 18

Holocene climatic variation recorded in a speleothem from McFail's Cave, New York
Philip E. van Beynen, Henry P. Schwarcz, and Derek C. Ford 20

Limnodrilus hoffmeisteri (Annelida: Oligochaeta: Tubificidae) in Pop's Cave, Wisconsin, USA
Hope Swayne, Mick Day, and Mark J. Wetzel 28

Cave Science News 32

The *Journal of Cave and Karst Studies* (ISSN 1090-6924, CPM Number #40065056) is a multi-disciplinary, refereed journal published three times a year by the National Speleological Society, 2813 Cave Avenue, Huntsville, Alabama 35810-4431 USA; (256) 852-1300; FAX (256) 851-9241, e-mail: nss@caves.org; World Wide Web: <http://www.caves.org/pub/journal/>. The annual subscription fee, worldwide, by surface mail, is \$18 US. Airmail delivery outside the United States of both the *NSS News* and the *Journal of Cave and Karst Studies* is available for an additional fee of \$40 (total \$58); The *Journal of Cave and Karst Studies* is not available alone by airmail. Back issues and cumulative indices are available from the NSS office. POSTMASTER: send address changes to the *Journal of Cave and Karst Studies*, 2813 Cave Avenue, Huntsville, Alabama 35810-4431 USA.

The *Journal of Cave and Karst Studies* is covered the the following ISI Thomson Services: Science Citation Index Expanded, ISI Alerting Services, and Current Contents/Physical, Chemical, and Earth Sciences.

Copyright © 2004 by the National Speleological Society, Inc. Printed on recycled paper by American Web, 4040 Dahlia Street, Denver, Colorado 80216 USA

Front cover: Calcite speleothems in stream bypass to the main stream passage of McFail's Cave, New York, in the Devonian Manlius Limestone. Photo by Art Palmer. See Philip E. van Beynen, Henry P. Schwarcz, and Derek C. Ford, p. 20.

Editor

Malcolm S. Field

National Center of Environmental Assessment (8623D)
Office of Research and Development
U.S. Environmental Protection Agency
1200 Pennsylvania Avenue NW
Washington, DC 20460-0001
202-564-3279 Voice 202-565-0079 FAX
field.malcolm@epa.gov

Production Editor

James A. Pisarowicz

Wind Cave National Park
Hot Springs, SD 57747
605-673-5582
pisarowicz@alumni.hamline.edu

BOARD OF EDITORS

Anthropology

Patty Jo Watson

Department of Anthropology
Washington University
St. Louis, MO 63130
pjwatson@artsci.wustl.edu

Conservation

Julian J. Lewis

J. Lewis & Associates, Biological Consulting
217 West Carter Avenue
Clarksville, IN 47129
812-283-6120
lewisbioconsult@aol.com

Earth Sciences-Journal Index

Ira D. Sasowsky

Department of Geology
University of Akron
Akron, OH 44325-4101
330-972-5389
ids@uakron.edu

Exploration

Paul Burger

Cave Resources Office
3225 National Parks Highway
Carlsbad, NM 88220
(505)785-3106
paul_burger@nps.gov

Life Sciences

Steve Taylor

Center for Biodiversity
Illinois Natural History Survey
607 East Peabody Drive (MC-652)
Champaign, IL 61820-6970
217-333-5702
sjtaylor@inhs.uiuc.edu

Paleontology

Greg McDonald

Geologic Resource Division
National Park Service
P.O. Box 25287
Denver, CO 80225
303-969-2821
Greg_McDonald@nps.gov

Social Sciences

Marion O. Smith

P.O. Box 8276
University of Tennessee Station
Knoxville, TN 37996

Book Reviews

Ernst H. Kastning

P.O. Box 1048
Radford, VA 24141-0048
ehkastni@runet.edu

Proofreader

Donald G. Davis

JOURNAL ADVISORY BOARD

Chris Groves	Carol Hill
Horton Hobbs III	David Jagnow
Julia James	Kathy Lavoie
Joyce Lundberg	Donald MacFarlane
	William White

EDITORIAL

MALCOLM S. FIELD

On January 1, 2004, Dr. Louise Hose resigned as Editor of the *Journal of Cave and Karst Studies* (JCKS) so that she could focus attention on her new duties as Director of the recently established National Cave and Karst Research Institute. As Editor for the past eight years, Dr. Hose managed several significant accomplishments with the *Journal*. Two accomplishments stand out, however. The first accomplishment was the elevation of the quality of papers published in JCKS, resulting in our recognition as one of the foremost karst journals in the world. The second accomplishment was the addition of JCKS to the Thomson ISI® services listing which includes Science Citation Index Expanded®, ISI Alerting Services®, and Current Contents® Physical, Chemical, and Earth Sciences® and distinguishes JCKS as the only karst publication currently sporting this distinction.

In December 2003, I accepted appointment as the new Editor of JCKS. My formal education focused on karst, and this focus has continued throughout my professional career. Currently, I am a senior research hydrogeologist for the U.S. Environmental Protection Agency in the Office of Research and Development where I am fortunate enough to be able to devote more than 90% of my time to karst-related issues. However, unlike most karst scientists who specialize in some aspect of speleogenesis, my interests are directed more toward addressing environmental problems associated with karstic terranes, particularly in terms of contamination of karstic aquifers and its attendant impacts on human health.



Learning all there is to know about editing JCKS is proving to be a substantial undertaking, but I am finding that good support is available to me with the assistance and advice of Dr. Louise Hose, Mr. Don Paquette, Dr. James Pisarowicz, Ms. Stephanie Searles, the *Journal* Associate Editors, and the Advisory Board from whom I am rapidly “learning the ropes,” as they say.

Although it will be exceedingly difficult to match the accomplishments of Dr. Hose, I intend to continue the dedication that is necessary for JCKS to maintain its status as one of the premier karst journals in the world. To this end, I have begun examining improvements such as a standard form for displaying tabular material which will be made avail-

able to prospective authors to facilitate table creation. To further assist authors in manuscript preparation, a set of templates conforming to the JCKS manuscript style is being developed for the most popular document-preparation platforms which include MS Word®, WordPerfect®, and LaTeX.

I would like to encourage prospective authors to consider submitting their manuscripts to JCKS. A review of past issues suggests a dearth of good exploration, social science, and conservation papers. It is my firm opinion that National Speleological Society (NSS) members will welcome papers addressing these topics as much as those more commonly represented in JCKS. I look forward to serving the NSS community and sharing in the knowledge that we are all striving to increase our understanding of caves and karst while working to preserve and protect our valuable karstlands.

APPLICATION OF HIGH-RESOLUTION X-RAY COMPUTED TOMOGRAPHY IN DETERMINING THE SUITABILITY OF SPELEOTHEMS FOR USE IN PALEOCLIMATIC, PALEOHYDROLOGIC RECONSTRUCTIONS

PATRICK J. MICKLER, RICHARD A. KETCHAM, MATTHEW W. COLBERT AND JAY L. BANNER
Department of Geological Sciences, The University of Texas at Austin, Austin, TX 78712-0254 USA

The isotopic and elemental compositions of speleothems can be used as proxies to elucidate past climate changes. Speleothem material is precious, however, and its use in such climate studies must be balanced against the need to preserve fragile cave environments. Accordingly, accurate assessment of the internal speleothem stratigraphy can provide insight into: 1) Overall sample quality for paleoclimate studies, and 2) the position of the central growth axis of the sample prior to destructive sample preparation, which involves bisecting by sawing the sample along its growth axis. Chemical and isotopic samples taken along the growth axis have the greatest potential to reflect the composition of the water from which the speleothem precipitated. The growth axis of speleothems cannot be reliably determined by visual inspection of uncut specimens, and incorrect bisections may compromise their applicability as geochemical climate proxies.

High-resolution X-ray computed tomography (HRXCT) is a non-destructive technique that can identify the position of the growth axis in speleothems by detecting subtle changes in calcite density between growth bands. HRXCT imagery of these variations can be animated as 'stacks' of slices and rendered in three dimensions. Such imagery can be used to identify the best plane along which the speleothem should be sectioned for sampling. These images may also reveal samples that have been extensively altered during their history, making them unsatisfactory for climatic studies. Additionally, HRXCT imagery can be used to determine the volume and location of large fluid inclusions for use in reconstructing the H and O isotopic composition of paleoprecipitation.

The use of isotopic and trace element compositions of speleothems (i.e., secondary cements found in caves such as flowstones, stalagmites, and stalactites), has grown with the increased interest in climate change studies. Speleothems are effective proxies in paleoclimate studies for several reasons, including the following: 1) they contain trace element and isotopic tracers that have been used to infer changes in paleotemperature, paleovegetation and paleoprecipitation (Hendy & Wilson 1968; Dorale *et al.* 1992; Winograd *et al.* 1992; Banner *et al.* 1996; Baker *et al.* 1998; Genty *et al.* 1998); 2) they may be continuously deposited over thousands of years and have thin growth bands that can be precisely dated using U-series dating methods (Musgrove *et al.* 2001); 3) growth rates of these bands may provide proxies for environmental parameters such as aquifer recharge rates (Proctor *et al.* 2000; Polyak & Asmerom 2001; Tan *et al.* 2003), and 4) speleothems form in a wide variety of locations where other high-resolution climate records may be absent. Although the potential value of speleothems in climate studies is clear, geochemical sampling is destructive, such that speleothem use should be balanced with the need to conserve fragile cave environments and material.

A speleothem is usually prepared for sampling by slicing the specimen, with a rock saw, along the growth axis and polishing the slabbed surface. The elemental and isotopic compo-

sition of speleothems may change away from the growth axis due to changes in water chemistry caused by progressive CO₂ degassing, evaporation and calcite precipitation (Hendy & Wilson 1968; Hendy 1971; Gonzalez & Lohmann 1988). Specifically, off-axis samples are more subject to non-equilibrium fractionation effects that are not regular or predictable. In addition, recent studies have attributed paleo-environmental significance to changes in speleothem growth band thickness (Proctor *et al.* 2000; Polyak & Asmerom 2001; Tan *et al.* 2003). Growth bands in speleothems thin away from the growth axis. For these reasons, acquisition of the most reliable paleo-environmental information requires that speleothems be sectioned to intersect the growth axis. Unfortunately, the growth history of speleothems is often complex (Fig. 1), making external visual identification of the growth axis difficult or impossible. A mistake during slabbing wastes valuable speleothem material and may limit data quality.

Computed tomography (CT) is a non-destructive technique for creating images of the interior of solid opaque objects (Ketcham & Carlson 2001). Rather than conventional X-radiography, in which an X-ray cone beam is projected through an entire sample onto film, CT images are created by directing a planar fan beam at an object from multiple angular orientations. The resulting images are termed slices because they correspond to what would be observed if the object were cut open

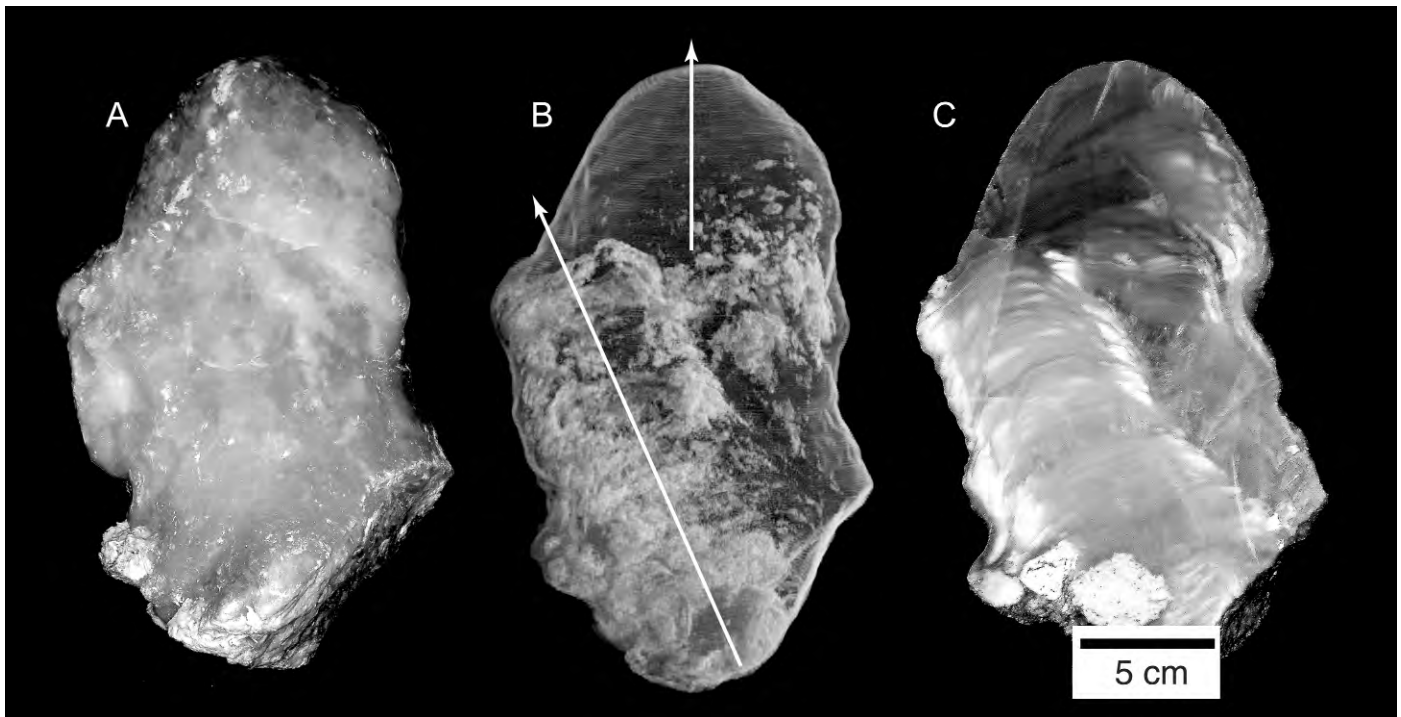


Figure 1. A. Photograph of the unsliced, unpolished side of stalagmite sample AH-M. Note that no internal structure is visible. B. Three-dimensional volume rendering of AH-M with solid material rendered transparent and inclusions rendered in lighter grays. Solid arrows indicate two different growth axes easily visible in the HRXCT data. The speleothem apparently leaned to one side during its growth, shifting the locus and apparent direction of precipitation. These images are available as a complete animation at: <http://www.ctlab.geo.utexas.edu/pubs/mickleretal/mickleretal.htm>. C. Photograph of the sliced and polished stalagmite AH-M. Note how the internal stratigraphy identified by HRXCT scanning prior to the slicing of the sample matches the stratigraphy of the polished specimen. The scan was used to identify the plane that intersected both growth axes.

along the image plane. The grayscales in these images correspond to relative X-ray attenuation, which is a function of elemental composition and density. By obtaining a series of contiguous slices for an object, a complete three-dimensional volume can be imaged. Because the fan beam has a thickness determined by the X-ray spot size and detector vertical pitch or collimation, the pixels in CT images are called voxels, or volume elements. Resolution in CT images is partly determined by the voxel dimensions, and partly by properties of the features being imaged.

High-resolution X-ray CT (HRXCT) is an industrial adaptation of standard medical CT or CAT scan. It differs in that it can use higher-energy X-rays, finer detectors, and longer imaging times, allowing it to penetrate denser objects and achieve 1-3 orders of magnitude better resolution than medical devices (Ketcham & Carlson 2001). The scanner at The University of Texas at Austin can image objects up to 500 mm in diameter, with a height of up to 1500 mm. Slice thickness on large objects (in excess of 75 mm in diameter or 150 mm high) can be as low as 0.25 mm. For smaller objects, the minimum slice thickness is approximately 1/1000 of the cross-sectional diameter, and can be as low as 5 μm .

HRXCT provides a non-destructive means to image the internal stratigraphy of speleothems, as it can detect density contrasts within the calcite growth bands. CT slices of these 'stratigraphic' variations can be animated as 'stacks' of slices, as well as rendered as a three-dimensional (3D) volume. The resulting imagery can serve as a guide to determine the most appropriate plane for sample sectioning and the overall suitability of the sample for study.

MATERIALS AND METHODS

SPECIMENS

Stalagmite AH-M was collected at the Apes Hill Quarry, Barbados, West Indies (Fig. 1 and 2). The stalagmite was unearthed from a cavity during quarry operations and subsequently donated to the University of Texas as part of an ongoing study of paleoclimatic and paleohydrologic reconstruction. The stalagmite is approximately 24 cm in height and 12 cm in diameter and consists of dense, optically clear calcite crystals. Like most speleothems, its shape and texture do not allow its internal stratigraphy to be ascertained.

Stalagmite ANY-01 (Fig. 3) was collected from Anyway Cave, Hays County, Texas for use in an ongoing study of pale-



Figure 2. HRXCT slice through AH-M showing density variations. Higher densities are indicated by lighter gray scale values. Two sets of concentric growth bands are visible. The upper set was apparently deposited before subsidence of the speleothem. The lower set indicates the location of the new growth axis on the flanks of the previously deposited speleothem material. A plane that bisects both growth axes is easily determined (dashed line A). A large void, near B, may be filled with air or the water from which this speleothem precipitated.

oclimatic and paleohydrologic reconstruction. The stalagmite is approximately 33 cm in height and 20 cm in diameter. Dark staining on the outside of the stalagmite, plus the reasons given above for AH-M, made determination of the internal stratigraphy impossible. Both stalagmite samples were CT scanned prior to sample preparation.

CT SCANNING

The specimens were scanned at the High-Resolution X-ray Computed Tomography (CT) Facility at The University of Texas at Austin (UTCT). The facility and typical scanning procedures and parameters are described in detail by Ketcham and Carlson (2001). Scanning parameters were optimized for fast

acquisition of slices, to minimize scanning time and costs. For sample AH-M, X-ray energy was set to 420 kV and 4.7 mA, with a focal spot size of 1.8 mm. X-rays were pre-filtered to reduce beam-hardening artifacts (artificial brightening of the edges compared to the center of the images caused by preferential attenuation of soft X-rays through dense objects) using two brass plates with a total thickness of 3.175 mm. X-ray intensities were measured using a 512-channel cadmium-tungstate solid-state linear array, with a horizontal channel pitch of 0.31 mm. Each slice was acquired using 808 views (angular orientations), each view having an acquisition time of 32 ms. The resulting acquisition time was approximately 34 seconds per slice. The speleothem was scanned in a 160% offset mode (Ketcham & Carlson 2001), with a slice thickness and inter-slice spacing of 1.0 mm. The image field of reconstruction was 180 mm, and the reconstructed image was created as a 512×512 16-bit TIFF file, resulting in an in-plane pixel resolution of 0.35 mm. Image reconstruction parameters were calibrated to maximize usage of the 12-bit range of grayscales available in the output images. Two hundred thirty nine images were obtained, with a total scanning time of approximately 2.25 hours.

For sample ANY-01, scanning parameters were changed slightly to accommodate the different sample dimensions. The differences were that the offset mode was 130%, there were 1000 views per slice, slice thickness and spacing were 2.0 mm and the field of reconstruction was 155 mm. One hundred fifty three slices were acquired, and the total scan time was approximately 1.75 hours.

Overall costs were \$200-\$300 per sample scanned. While not trivial, such amounts are small compared to the time and expense of field work and geochemical analysis, in addition to the larger issues of data quality and preservation of cave material. It should also be emphasized that data with better clarity and resolution than those presented here can be obtained with the equipment used for this study, if greater detail is required for a particular research objective.

IMAGE PROCESSING

Animations of the original CT serial sections were made using QuickTime™. Two techniques were used to study the data in three dimensions. First, images were ‘resliced’ along orthogonal planes using ImageJ© creating a series of images that can be animated. This software program can be downloaded from the National Institutes of Health (NIH) web site (<http://rsb.info.nih.gov/ij/>). Second, a technique known as volume rendering was used to create visualizations of the entire data volume in three dimensions. Volume rendering consists of allocating to each voxel grayscale value a color and opacity, allowing some materials to be transparent while leaving others partially or fully opaque, while also retaining the density information in the images. The entire data set can be rendered, or a part can be cut away along an arbitrary plane to reveal any internal surface. These renderings were accomplished using VG Studio Max™ software (Volume Graphics GmbH, Heidelberg, Germany).



Figure 3. Volume renderings of ANY-01. Cutaways reveal a late shift in the primary growth axis and significant internal porosity around the growth axis. Calcite deposited after the shift in the growth axis has a significantly lower porosity and higher density than calcite near the core of the speleothem. This calcite drape further complicates the visual inspection of the speleothem by obscuring the highly porous central core.

RESULTS AND DISCUSSION

CT scanning of the speleothems reveals complex internal stratigraphies that can not be identified by visual inspection of the uncut specimens. For sample AH-M, CT scanning revealed that the locus of deposition changed significantly at least three times as the stalagmite leaned to one side during its growth (Fig. 1). This stratigraphy likely resulted from deposition on a soft substrate that settled during formation of the stalagmite.

Similar to AH-M, CT scanning of ANY-01 reveals that the latest stage of growth took place off the main axis (Fig. 3). Additionally, the late stage calcite is denser than the previously deposited calcite and formed a drape on the outside of the stalagmite, which obscures the porous nature of the underlying calcite. CT scanning reveals the multiple growth axes of these stalagmites and the planes that intersect these axes (Fig. 2).

In addition to aiding in the identification of the growth axes, CT scanning also reveals the volume and location of large voids within the stalagmite, which may be filled with air or water (Fig. 2). Researchers have recently analyzed water from large fluid inclusions in speleothems for use in paleoprecipitation stable-isotope reconstructions (Genty *et al.* 2002). The dramatic density contrast between calcite and pore space (either water- or air-filled) allows easy identification of voids that fall within the scan's scale of resolution. A more time-intensive scanning protocol with detailed calibration could potentially allow discrimination between fluid-filled and air-filled voids, although this was not undertaken in this study because the primary objective was inexpensive inspection for growth axis determination.

The scanning reveals that AH-M is comprised of dense calcite with an occasional isolated void. In contrast, the calcite around the primary growth axis of ANY-01 varies greatly in density and contains many large and small voids (Fig. 3). Porous calcite around the growth axis of a speleothem may allow both post-depositional alteration of calcite through isotopic and elemental exchange with cave water, and emplacement of pore-filling calcite cements. Such processes will alter the primary isotopic and elemental composition of a speleothem, rendering it unsuitable for paleoclimate studies. For these reasons, ANY-01 was not sliced for sampling. Where feasible such samples can be returned to the location within the cave from which they were collected.

Another feature of CT imagery is that it can be easily disseminated via the Internet, both as a record of the work done and potentially as an educational or archival resource. Web-based images allow remote users to view CT data animations, isolate individual slices, and view rendered 3D volumes from any orientation. Scans and image processing of the samples used in this study are available on the World Wide Web at: (<http://www.ctlab.geo.utexas.edu/pubs/mickleretal/mickleretal.htm>).

ACKNOWLEDGEMENTS

We would like to thank the management at Williams C. O. Asphalt and Quarries LTD. for providing access to Apes Hill Quarry, Barbados, West Indies and Dr. George Veni and Mr. David Buie for providing the sample ANY-01 from Anyway Cave, Hays County, Texas, USA. We thank Dominique Genty, an anonymous reviewer, and Earth Science Editor Dr. Ira D. Sasowsky for constructive comments.

REFERENCES

- Baker, A., Genty, D., Dreybrodt, W., Barnes, W.L., Mockler, N.J., & Grapes, J., 1998, Testing theoretically predicted stalagmite growth rate with recent annually laminated samples; implications for past stalagmite deposition: *Geochimica et Cosmochimica Acta*, v. 62, no. 3, p. 393-404.
- Banner, J.L., Musgrove, M., Asmerom, Y., Edwards, R.L., & Hoff, J.A., 1996, High-resolution temporal record of Holocene ground-water chemistry; tracing links between climate and hydrology: *Geology*, v. 24, no. 11, p. 1049-1053.
- Dorale, J.A., Gonzalez, L.A., Reagan, M.K., Pickett, D.A., Murrell, M.T., & Baker, R.G., 1992, A high-resolution record of Holocene climate change in speleothem calcite from Cold Water Cave, Northeast Iowa: *Science*, v. 258, no. 5088, p. 1626-1630.
- Genty, D., Plagnes, V., Causse, C., Cattani, O., Stievenard, M., Falourd, S., Blamart, D., Ouahdi, R., & Van-Exter, S., 2002, Fossil water in large stalagmite voids as a tool for paleoprecipitation stable isotope composition reconstitution and paleotemperature calculation: *Chemical Geology*, v. 184, no. 1-2, p. 83-95.
- Genty, D., Vokal, B., Obelic, B., & Massault, M., 1998, Bomb ^{14}C time history recorded in two modern stalagmites; importance for soil organic matter dynamics and bomb ^{14}C distribution over continents: *Earth and Planetary Science Letters*, v. 160, no. 3-4, p. 795-809.
- Gonzalez, L.A., & Lohmann, K.C., 1988, Controls on mineralogy and composition of spelean carbonates; Carlsbad Caverns, New Mexico, *in* James, N.P. & Choquette, P.W. (eds.), *Paleokarst*. Queen's University, Kingston, Ontario, Canada, p. 81-101
- Hendy, C.H., 1971, The isotopic geochemistry of speleothems; 1, The calculation of the effects of different modes of formation on the isotopic composition of speleothems and their applicability as paleoclimatic indicators: *Geochimica et Cosmochimica Acta*, v. 35, no. 8, p. 801-824.
- Hendy, C.H., & Wilson, A.T., 1968, Palaeoclimatic data from speleothems: *Nature*, v. 219, no. 5149, p. 48-51.
- Ketcham, R.A., & Carlson, W.D., 2001, Acquisition, optimization and interpretation of X-ray computed tomographic imagery; applications to the geosciences: *Computers & Geosciences*, v. 27, no. 4, p. 381-400.
- Musgrove, M., Banner, J.L., Mack, L.E., Combs, D.M., James, E.W., Cheng, H., & Edwards, R.L., 2001, Geochronology of late Pleistocene to Holocene speleothems from central Texas: Implications for regional paleoclimate: *Geological Society of America Bulletin*, v. 113, no. 12, p. 1532-1543.
- Polyak, V.J., & Asmerom, Y., 2001, Late Holocene climate and cultural changes in the southwestern United States: *Science*, v. 294, no. 5540, p. 148-151.
- Proctor, C.J., Baker, A., Barnes, W.L., & Gilmour, M.A., 2000, A thousand year speleothem proxy record of North Atlantic climate from Scotland: *Climate Dynamics*, v. 16, no. 10/11, p. 815-820.
- Tan, M., Liu, T.S., Hou, J., Qin, X., Zhang, H., & Li, T., 2003, Cyclic rapid warming on centennial-scale revealed by a 2650-year stalagmite record of warm season temperature: *Geophysical Research Letters*, v. 30, no. 12, p. 1617.
- Winograd, I.J., Coplen, T.B., Landwehr, J.M., Riggs, A.C., Ludwig, K.R., Szabo, B.J., Kolesar, P., & Revesz, K.M., 1992, Continuous 500,000-year climate record from vein calcite in Devils Hole, Nevada: *Science*, v. 258, p. 255-258.

COMPARISON OF A NEW GIS-BASED TECHNIQUE AND A MANUAL METHOD FOR DETERMINING SINKHOLE DENSITY: AN EXAMPLE FROM ILLINOIS' SINKHOLE PLAIN

JULIE C. ANGEL, DANIEL O. NELSON, AND SAMUEL V. PANNO

Illinois State Geological Survey, Natural Resources Building, 615 E. Peabody Dr., Champaign, IL 61820-6964 USA

A new Geographic Information System (GIS) method was developed as an alternative to the hand-counting of sinkholes on topographic maps for density and distribution studies. Sinkhole counts were prepared by hand and compared to those generated from USGS DLG data using ArcView 3.2 and the ArcInfo Workstation component of ArcGIS 8.1 software. The study area for this investigation, chosen for its great density of sinkholes, included the 42 public land survey sections that reside entirely within the Renault Quadrangle in southwestern Illinois.

Differences between the sinkhole counts derived from the two methods for the Renault Quadrangle study area were negligible. Although the initial development and refinement of the GIS method required considerably more time than counting sinkholes by hand, the flexibility of the GIS method is expected to provide significant long-term benefits and time savings when mapping larger areas and expanding research efforts.

Sinkholes, the most diagnostic surface expression of karst landscapes, can be found extensively throughout the world. Approximately 7-10% of the earth's surface has been classified as karst terrane, and more than 25% of the world's population obtains its water supply from karst aquifers (Ford & Williams 1992). Sinkholes provide direct routes for surface water to drain into the underlying karst aquifer. This rapid drainage allows little time for the natural filtration and biodegradation processes that naturally occur in non-karst areas (White 1988). The result is contamination of groundwater resources with bacteria from human and animal sources (Panno *et al.* 1997a; 2003), agrichemicals from row crop production (Waite & Thomson 1993; Panno *et al.* 2003), as well as chemicals that have been spilled or dumped on the surface (Waite & Thomson 1993). Sinkholes also present potential hazards for land use, contributing to soil collapse and erosion by conveying soil underground (Hyatt & Jacobs 1996). Existing and future structures such as commercial and residential developments, transportation infrastructures, and waste disposal sites in karst terranes are at risk for damage from subsidence. Sinkhole density maps depicting the number of sinkholes per unit area provide useful information for determining areas of greatest risk for karst-related groundwater contamination and subsidence.

Sinkhole density maps can be used as a precursor to dye-tracing studies to identify groundwater flow paths and to locate the boundaries of groundwater basins. Panno and Weibel (1999) showed that mapping of sinkhole distribution, sinkhole density, and sinkhole area yielded an approximation of groundwater basin boundaries within the sinkhole plain of southwestern Illinois. Subsequent dye-tracing experiments in this area by Aley *et al.* (2000) used these preliminary maps as a basis for the selection of dye injection points.

Our work is based on sinkholes identified on a 1:24,000 USGS topographic map of the Renault Quadrangle with a contour interval of 20 feet. Applegate (2003) found more sinkholes during karst field observations in the Mt Airy Forest of Hamilton County, Ohio than were indicated on 1:24,000 USGS maps of that area. The study found that sinkhole recognition on contour maps is limited by sinkhole size, map scale, contour interval, and slope.

Gathering and analyzing sinkhole data for sinkhole density studies in mature karst regions has historically required the tedious, time-consuming process of manually counting sinkholes shown on topographic maps. In areas containing thousands to tens of thousands of sinkholes, this manual method requires a significant amount of time, and the patience for careful visual scanning of paper maps to avoid miscounting of sinkholes. We devised a GIS-based method to provide an alternative to hand-counting sinkholes as well as additional applications for karst research and management (e.g., by comparing sinkhole layers with geologic and infrastructure layers). GIS technology provides the means for analyzing the spatial distribution of geographic information, modeling its interactions, and finding patterns and relationships in the data that may be overlooked by previously-used techniques (Szukalski 2002).

SOUTHWESTERN ILLINOIS' SINKHOLE PLAIN

The sinkhole plain, which covers parts of three counties in southwestern Illinois (Fig. 1), contains over 10,000 sinkholes and numerous caves and springs (Panno *et al.* 1997b). The Renault Quadrangle was chosen for this investigation because of its particularly high density of sinkholes (Fig. 2). The study area is on the southwestern flank of the Illinois Basin where Mississippian-age rocks crop out and subcrop under thin

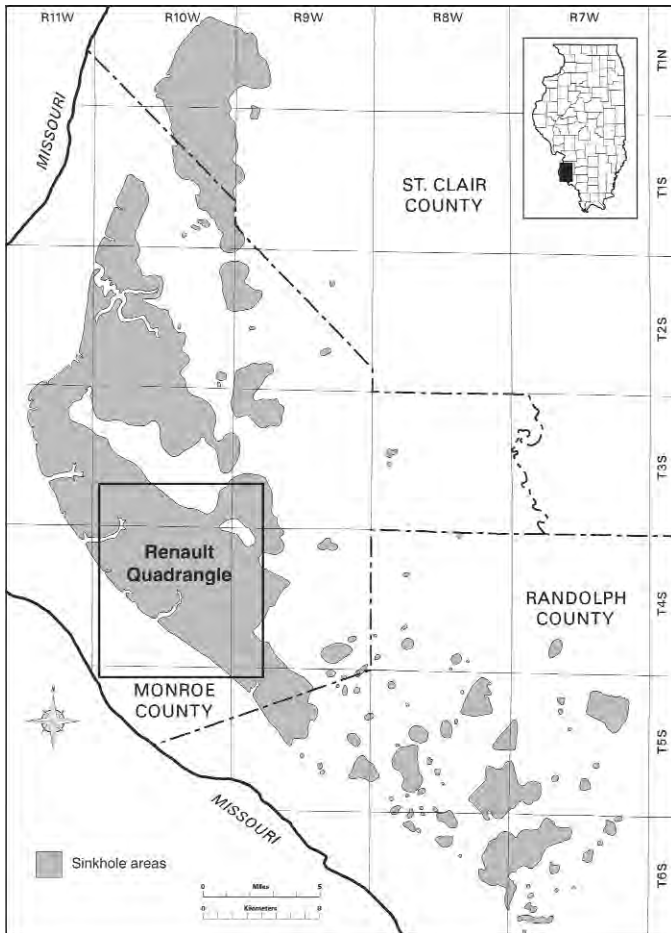


Figure 1. Map showing the location of the Renault Quadrangle within the karst terrane of the southwestern Illinois sinkhole plain, modified from Panno *et al.* (2001)



Figure 2. Aerial view of a typical area within the southwestern Illinois sinkhole plain adjacent to the bluffs of the Mississippi River looking west. Sinkholes are marked by depressions, tree clusters, and ponds. Photograph by Joel Dexter, ISGS, 2000.

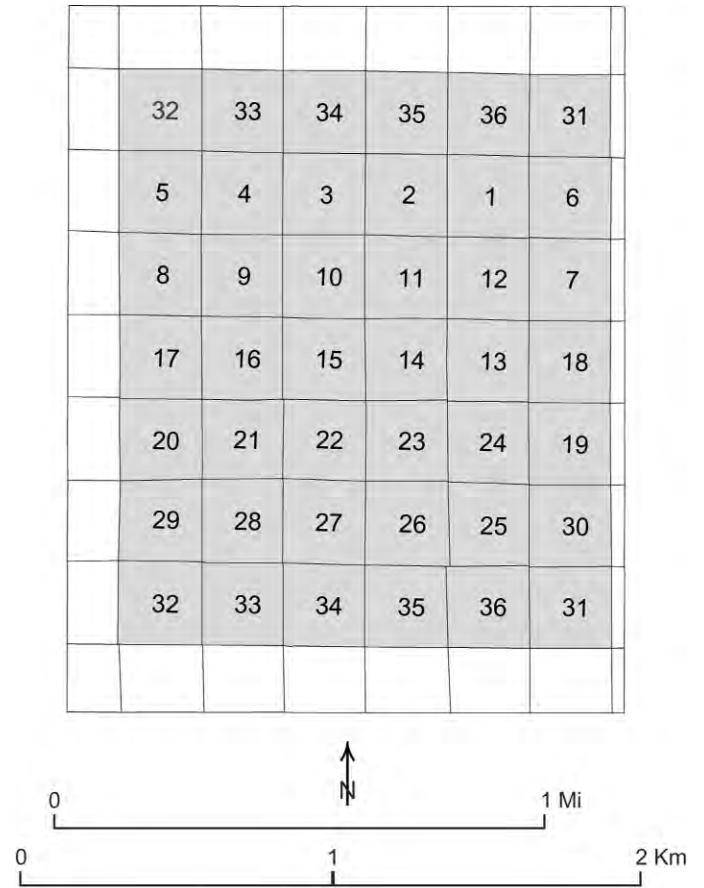


Figure 3. Map of the Renault Quadrangle showing the 42 public land survey sections. Only whole sections (shaded gray, with section number) were included in the study area.

glacial drift and wind-blown loess (Panno *et al.* in press). The main karst-forming formation that underlies much of the sinkhole plain and the Renault Quadrangle is the St. Louis Limestone (Willman *et al.* 1975).

The population of Monroe County, where the Renault Quadrangle is located, has grown by 23.2% from 1990 to 2000 (U.S. Census Bureau 2000). This rapid growth is largely due to urban expansion from the St. Louis metropolitan area. The high degree of karstification, combined with the rapid increase in population, presents many challenges for public officials in protecting groundwater resources and emphasizes the need for sinkhole density and distribution studies to aid in community planning and development.

METHODS

We used ArcView 3.2 and the ArcInfo Workstation component of ArcGIS 8.1 software to create a new GIS-based method that provides an alternative to the hand-counting of sinkholes for density and distribution studies. Sinkhole counts prepared by hand from the printed quadrangle map were compared to

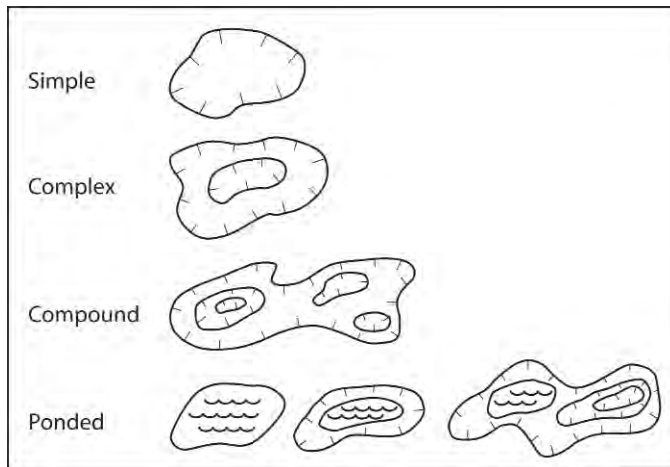


Figure 4. Examples of the four common sinkhole forms in the study area: simple sinkhole – defined by a single, non-nested depression contour; complex sinkhole – defined by one set of nested contours; compound sinkhole – defined by multiple nested depression contours; and ponded sinkholes which can appear as a water body without a depression contour, as ponded water within a simple sinkhole, or as a water body within a compound or complex sinkhole (example shown is within a compound sinkhole). Modified from White, 1988.

those generated by the GIS-based method from USGS Digital Line Graphs (DLGs) of the Renault Quadrangle. GIS methods have previously been used to produce karst maps, to analyze sinkhole density for karst evolution studies (Denizman & Randazzo 2000), for water resource protection (Waite & Thomson 1993), and for inventorying karst features to provide land-use planners and municipalities with data needed for decision making (Kochanov 1999; Brezinski & Dunne 2001; Green *et al.* 2002). Although these studies utilized GIS software, none examined the differences and potential errors that may be involved in using GIS-based techniques to obtain sinkhole counts for density and distribution studies. This investigation examines the possible differences and discrepancies through direct comparison of sinkhole counts obtained from GIS methods with counts obtained from standard manual methods.

The study area used in this investigation included 42 public land survey sections that reside entirely within the Renault Quadrangle of southwestern Illinois (Fig. 3). The partial sections that intersect the quadrangle perimeter were omitted to eliminate the complexities of accounting for incomplete sinkhole counts in these sections.

CLASSIFICATION AND DEFINITION OF SINKHOLE FEATURES

Sinkhole morphology in the Renault Quadrangle is varied, resulting in the need to classify and define those features to be considered for sinkhole counts. Four common types of sinkholes are present in this region: simple, complex, compound, and ponded sinkholes (Fig. 4). Simple sinkholes are defined as

having a single, non-nested depression contour, whereas complex sinkholes appear as simple sinkholes, but have two or more nested depression contours. Compound sinkholes are defined as large, irregularly-shaped depression contours with two or more sets of nested depression contours. Ponds that do not appear to be man-made are defined as sinkholes; these circular or elliptical bodies are generally soil-and debris-plugged depressions that retain water. Ponded sinkholes appear as a body of water without a depression contour, as ponded water within a simple sinkhole, or as a water body within a complex or compound sinkhole.

HAND-COUNTING SINKHOLES BY WHOLE SECTION

Sinkholes were counted by hand for each whole section and summed to the nearest quarter sinkhole using a printed copy of the 7.5-minute, 1:24,000-scale, U.S. Geological Survey (USGS) map of the Renault Quadrangle, Monroe County, IL (USGS 1993a). Sinkhole counts were compiled by summing the number of simple and ponded sinkholes, and each of the innermost depression contours within the complex and compound sinkholes (Fig. 5).

Section 4 of the Renault Quadrangle study area (Fig. 6) exemplifies the varied sinkhole features that were considered when generating sinkhole counts. The southwest quarter of the section includes several simple sinkholes, ponded sinkholes, and a man-made pond. The large sinkhole in the center of the southeast quarter is an example of a compound sinkhole, displaying four distinct innermost depression contours, yielding a count of four individual sinkholes. A large complex sinkhole can be seen just below the section label. Several sinkholes can be seen overlapping the southern section line of Figure 6, demonstrating the need for a consistent method of counting sinkholes that overlap section boundaries. During hand-counting, each overlapping sinkhole was apportioned to multiple sections by estimating, to the nearest quarter, the area of the sinkhole within a given section. The partial sinkhole counts added 3.25 sinkholes to the 63 complete sinkholes fully contained within the section, yielding a section count of 66.25 sinkholes.

Each sinkhole was highlighted as it was counted to ensure that each was counted only once. This procedure was followed for each complete section in the Renault Quadrangle. Several sections in the study area had incomplete section lines. These were sketched in by hand to delineate each section and to assign sinkhole counts to the appropriate section. The missing section lines were the result of French colonization land grants and old Indian treaty boundaries that were honored upon establishment of the newer township and range system (Cote 1972). Partial sections along the boundaries of the quadrangle map were not included in this study to eliminate the complexities of accounting for incomplete sinkhole counts in the affected sections.

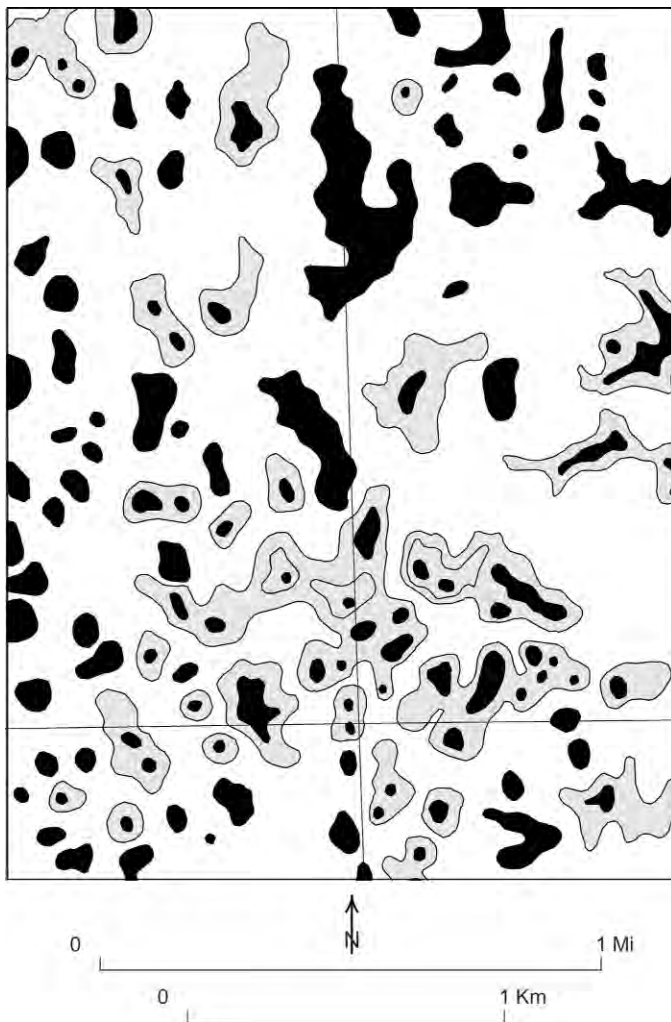


Figure 5. Map of a representative section of the Renault Quadrangle demonstrating what were considered sinkholes for this study. Areas in gray represent complex and compound sinkholes. Areas in black represent either simple sinkholes, ponded sinkholes, or the interior of the innermost depression contours of the complex and compound sinkholes. Each black area was counted as one sinkhole.

COMPUTER-GENERATED SINKHOLE COUNTS BY SECTION

To derive computer-generated sinkhole counts and related statistics by section, an ArcView project was developed using ArcView 3.2 and the ArcInfo Workstation component of ArcGIS 8.1. The sinkhole data layer was generated for the Renault Quadrangle by combining the Digital Line Graph (DLG) hypsography and hydrography data layers with an Illinois Public Land Survey System (PLSS) data layer. All data were cast on the Universal Transverse Mercator (UTM) coordinate system, zone 15, and the North American Datum of 1983 (NAD83).

The hypsography DLG layer was obtained from the U.S. Geological Survey (1993b) and converted to the ArcInfo cov-

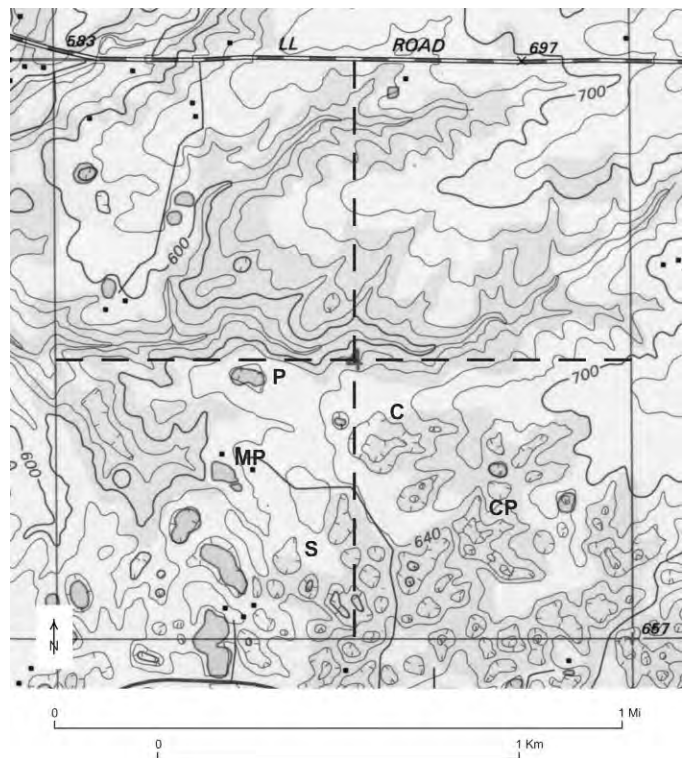


Figure 6. Section 4 of the Renault Quadrangle showing the variety of sinkhole features considered for hand counting. Examples of simple and ponded sinkholes appear in the southwest quarter section. A large compound sinkhole appears just below the center of the southeast quarter section. An example of a complex sinkhole can be seen just below the section label. S=simple, C=complex, CP=compound, P=sinkhole pond, MP=man-made pond. Modified from USGS topographic map of Renault Quadrangle, 1993.

erage format. Depression contours in the coverage were selected as those having DLG codes of major = 20 and minor = 611. A new field named “depression” was added to the coverage and the selected set was assigned a value of depression = 1, indicating that they were indeed depression contours. All other records were assigned a value of depression = 0, indicating that they were non-depression contours.

It was important to ensure that all depression contours represented fully closed polygons. The ArcEdit module of ArcInfo was used to check for any dangling nodes indicating depression contours that did not form closed polygons. Affected polygons were repaired by digitizing the missing portions of the polygons.

Depression polygons were identified in ArcView by using arcs previously labeled as depression boundaries. This was accomplished by using the non-depression contours to identify all non-depression areas, then switching the selection to select all depression areas. This counter-intuitive algorithm is based on the premise that a non-depression contour (e.g. line feature) can almost never be part of the perimeter of a depres-

sion area (e.g. polygon feature). Therefore, every polygon perimeter that is formed, at least in part, by a non-depression contour, must be a non-depression polygon. Switching the selection yields all areas that are depressions. A procedural step was included to check for any non-depression contours that might be imbedded in a depression, such as might occur if a small local high were found within a larger depression. None were expected and none were found to exist.

The Renault Quadrangle hydrography DLG layer (USGS 1993c) was added to identify additional water-filled depression features that were not present in the hypsography layer due to the 20-foot contour interval. A hydrography polygon coverage was prepared using the same methods as for the hypsography layer and a hydrography polygon theme was added to the database. This theme was constrained to only those polygons identified as water bodies (major value = 50), and a depression column was added to the theme's attribute table. Therefore, water bodies in the hydrography data set that were already accounted for in the hypsography data set were automatically removed from consideration. The remaining water bodies were assigned a hydrography depression value = 1. The subset was visually inspected to remove any hydrography features that were not formed by karst processes. These included man-made ponds, lakes or reservoirs, as well as any non-karst depressions present in the Mississippi River flood plain. These non-karst features were assigned a value of depression = 0.

At this point, the database contained the hypsography and hydrography data sets, each with a defined set of unique depressions. A source field was added to each of the two attribute tables as a means of identifying the source DLG for each depression record. A union was executed in ArcInfo to combine the two data sets into a single coverage that contained all depression polygons. After the coverage was built, polygon topology was verified and the coverage was checked for any label or node errors. The sinkhole attribute table was inspected to verify that polygon attributes were as expected, confirming that all polygons were labeled as depression = 1 and that each record contained a source column entry.

The next several procedures were perhaps the most important steps in the development of the method. In the hand-counting method, sinkhole counts were compiled by counting the number of simple and ponded sinkholes, as well as the innermost depression contours of complex and compound sinkholes. The first step to derive similar counts using GIS methods was to identify the singular, complex, and compound depression polygons within the sinkhole data layer. This was accomplished in ArcInfo by merging all nested polygons in the sinkholes coverage and creating a new coverage called "compound" that contained all outer boundaries of the compound and complex depressions plus the simple and ponded depression polygons. The compound arcs feature class was added to the ArcView project and used to select all adjacent depression polygons. This produced the set of depression polygons that included all the outer polygonal rings of the complex and compound depression polygons, and all the simple and ponded

Goal

Populate a data field called "interior" which indicates the nesting level values for all nested polygons in a complex or compound depression and identifies the polygons that participate in a complex or compound sinkhole.

Assumptions and constraints

- A set of nested polygons may have 1 to many nesting levels.
- The series (0 to n) for any set of nested polygons is an uninterrupted, continuous sequence of positive integers that increment by 1.
- Non-nested polygons and the outermost polygon of the complex and compound depressions will have nesting values of zero.
- The remaining polygons have an initial interior value of interior = 1.

Algorithm

- Set n equal to the initial interior value assigned to all the components of the nested polygons in the data set (n=1)
 - Start Loop: For each value of n, from n to maximum nested level, by increments of +1, do the following:
 - In ArcInfo:
 - Dissolve sinkholes interior<n> interior poly
 - Build interior<n> line
 - In ArcView:
 - Add interior<n> arcs to view
 - Select interior<n> arcs
 - Select polygons from sinkholes theme adjacent to the selected set
 - Open sinkholes table and switch selection
 - Select from set, interior > 0
 - Calculate selected set to interior = n + 1
 - Save/Close ArcView
 - Increment n (i.e. n = n + 1)
 - Loop
 - Select sinkhole theme polygons with interior <> 0
 - Select features of active theme that intersect selected sinkholes features
 - Calculate comp = 1
- [End]

Figure 7. Selection algorithm A for determining the interior nesting levels of all complex and compound polygons within sinkhole areas.

polygons. By switching the selection, all polygons that represented the interior components of the complex and compound depression were isolated. A field named "comp" was added, and all interior components of the complex and compound depressions were assigned a comp value = 1. A field named "interior" was added, and all interior components of the selected set were assigned a value of interior = 1 to identify them as part of a complex or compound sinkhole.

It was necessary to determine the interior nesting levels of the complex and compound depressions to ultimately identify the innermost depression polygons to be counted as sinkholes. Complex and compound depressions could contain several sets of nested polygons, making it possible for these nested depressions to have several innermost polygons. Interior nesting levels were determined using algorithm A (Fig. 7). The result was that each complex or compound depression had a series of nested pseudo-concentric rings. The rings were labeled in

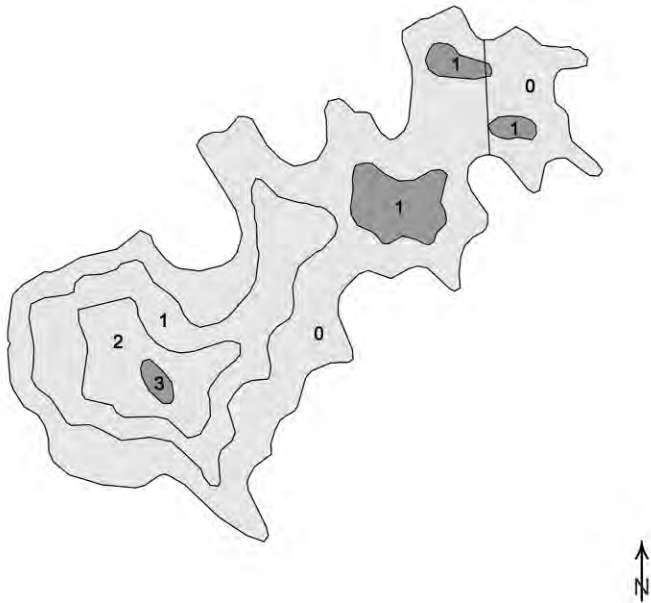


Figure 8. Compound sinkhole with labeled nesting levels. Outermost nested polygon is labeled 0. Innermost is labeled 3. The four darker polygons, one labeled 3 and three labeled 1, were counted as sinkholes as each is locally innermost. Note also the section line that divides the northeast lobe. The uppermost interior polygon is apportioned between two sections.

ascending order where zero was the outermost ring and “n”, with a maximum value of three (Fig. 8), was the innermost.

Singular depressions were defined as simple and ponded depressions, and the innermost polygons of any complex or compound depression. Identifying these singular depressions in ArcView produced the set from which sinkhole counts were ultimately derived. Algorithm B (Fig. 9) illustrates the singular depression selection process.

Unique ID values were assigned to each polygon in the sinkhole attribute table. To identify the nested polygon components of any complex or compound polygon set, compound IDs were assigned to each set by first transferring the unique IDs of any complex or compound component to the compound coverage, then spatially joining the sinkhole and compound coverages. This join enabled the transfer of all complex and compound IDs to the interior nested polygons, providing a means for identifying all the components of any complex or compound sinkhole, either as an individual polygon or as a component of the compound group. This completed the generation of a thoroughly attributed sinkhole coverage.

The final step in preparing the data for analysis involved intersecting sinkhole data with township, section, and range data for the quadrangle. Adding township, section, and range parameters to the sinkhole polygon attributes table provided the means to apportion sinkholes divided by section lines into the appropriate sections.

To obtain sinkhole counts per section, it was necessary to

Goal

Populate a data field called "singular" which indicates whether or not a polygon is the innermost of a nested set of polygons, or a simple or ponded polygon. An innermost, simple or ponded polygon will be set to singular= 1, otherwise it will be set to singular= 0.

Assumptions and constraints

- The nesting level values for all polygons have already been determined and assigned to a data field called "interior".
- The outermost polygon of a set of nested polygons has a nesting level value of zero (interior = 0).
- The innermost polygon of a set of nested polygons has a nesting level of n, where n is a positive integer.
- The series (0 to n) for any set of nested polygons is an uninterrupted, continuous sequence of positive integers that increment by 1.
- A set of nested polygons may have 1 to many innermost polygons. For example, a complex sinkhole of large size may have several sets of nested depression polygons contained within the overall area of depression.

Algorithm

- Set n equal to the maximum value of "interior" for the set of all nested polygons in the entire data set.
 - Select the set of polygons that have interior = n
 - Start Loop: For each value of n, from n to 0, by increments of -1, do the following:
 - Set singular = 1 for the selected set
 - Select a new set of polygons having interior >= n
 - Select the set of polygons adjacent to the selected set
 - Switch the selected set (non-selected become selected and vice versa)
 - Decrement n (i.e., $n = n - 1$)
 - Reselect from the current set the subset of polygons with interior = n
 - Loop
 - Clear selected set
 - Select comp = 0
 - Set singular = 1 for selected set
 - Select the set of all polygons that have singular = 1
 - Switch the selected set (non-selected become selected and vice versa)
 - Set singular = 0 for the selected set
- [End]

Figure 9. Selection algorithm B for determining the set of innermost polygons from a set of nested polygons representing elevation contour ranges within sinkhole areas, and the simple and ponded polygons.

obtain a “countable” value for the partial sinkhole components that overlap section lines. This was accomplished by relating the total area of any overlapping sinkhole to the areas of its partial components and deriving a value between 0 and 1. Total area values for individual sinkholes were determined by summing area by unique ID in the sinkhole attribute table. The resulting summary table was joined to the sinkhole attribute table based on the unique ID value. A weighted count for each sinkhole was derived by dividing the area of the partial component by the area of the entire sinkhole. Sinkhole counts per section were finalized by selecting the set of sinkholes having singular = 1 (countable sinkholes), and summing the weighted count by township, section, and range. A total sinkhole count

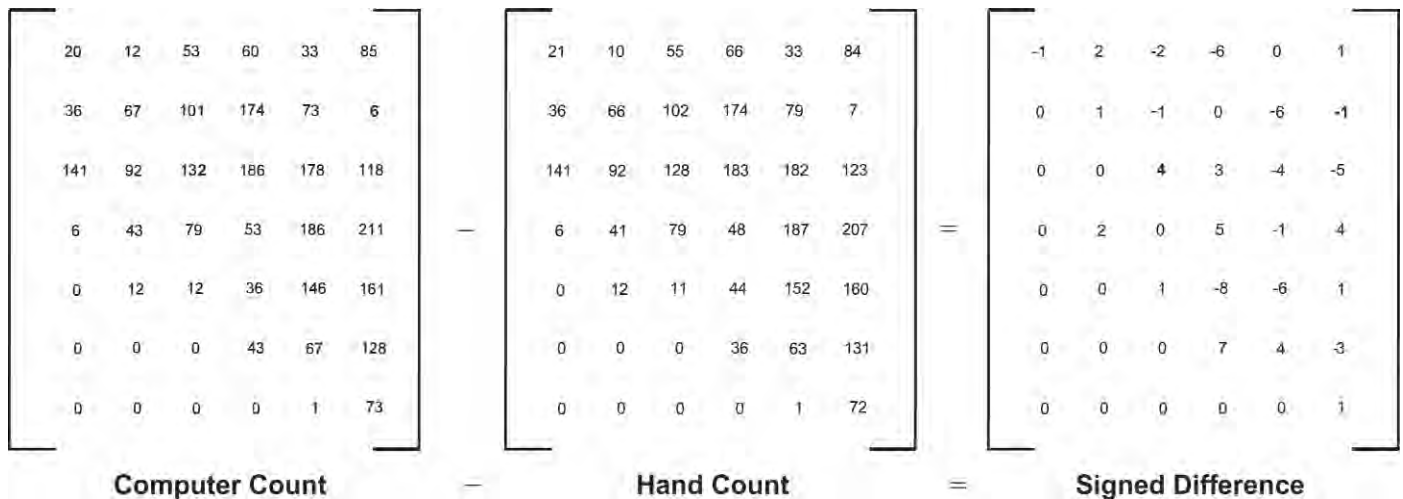


Figure 10. Matrix representation of computer counts minus hand counts and the resulting differences for each section in the study area. Section counts were rounded to the nearest whole number.

for the entire Renault study area was derived by summing all the weighted counts.

ANALYSIS AND COMPARISON OF COUNTING METHODS

Sinkhole counts from the GIS database totaled 2,823 within the study area, while 2,830 sinkholes were counted manually using the paper map, yielding a negligible difference. Although the difference is small, potential sources of error were examined to reveal any shortcomings that may exist in either counting method.

Comparison of the computer- and hand-counts by section (Fig. 10) demonstrated differences that ranged from an over-count of 7 sinkholes to an under-count of 8 sinkholes by the GIS method relative to the hand-counted standard. Sinkholes were over-counted by the GIS method in 13 sections, under-counted in 12 sections, and matched the hand-counts in 12 sections. The remaining 5 sections, which were located completely within the Mississippi River floodplain, contained no sinkholes. The counting errors exhibited at the section level essentially cancelled each other out through summation, resulting in the small difference seen in the total study area counts for the two methods.

The total sinkhole counts for the study area completed by hand and by computer were compared using the Wilcoxon signed-rank test (Snedecor & Cochran 1989); a nonparametric test used as a substitute for the t-test for paired samples. The null hypothesis (the two populations of sinkhole counts are equal) was accepted ($P = 0.95$) on the basis of the test. That is, the results of the two counting methods were found to be statistically equivalent.

Sections with numerical discrepancies were examined in an attempt to determine causes of the disparities. Minor differences in counts for several sections occurred from differences in assigning proportional counts for those sinkholes that over-

lapped section lines. The GIS method is capable of exactly apportioning sinkholes split by section boundaries, whereas accurate apportionment for anything less than a quarter of a sinkhole is difficult to attain with hand-counting.

The addition of the hydrography data layer added desired ponded sinkholes to the database, however, unwanted man-made bodies of water were added as well. In this area, most man-made ponds can be identified by the appearance of a square edge that represents the dammed side of the pond, and were removed from both the paper map and the GIS database based on the presence of this feature. Identifying the squared sides of a man-made pond proved more difficult using GIS analysis due to the square nature of the digitized vectors that form the polygon boundaries. It was necessary to use the zoom feature to adequately view the smaller ponds, yet zooming tended to accentuate the square nature of the vectors. These difficulties with pond labeling caused several minor errors by removing sinkhole ponds or by failing to remove man-made ponds.

A slight difference in the locations of the missing section lines that were added became evident when comparing the digital- and hand-counts in the southeast quarter of the quadrangle. The absent section lines were added to the statewide digital Public Land Survey System (PLSS) layer when it was developed in the 1980s. The absent lines were drawn on the paper map during hand-counting. The slight locational discrepancies between these two versions of the added section lines would not have been discovered if not for the discrepancy they caused in sinkhole counts. This difference in line placement skewed the actual counts for sections on both sides of the lines, causing over- and under-counts that would not have been present had both lines been placed in the same map location.

Most of the discrepancies in section and overall counts were accounted for within the visual estimation errors of the

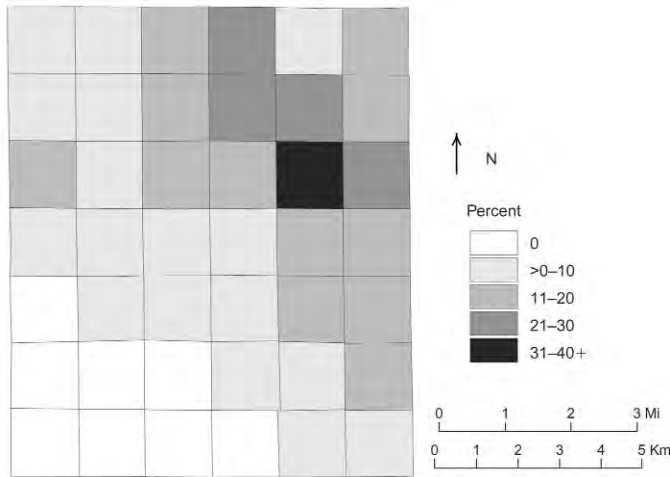


Figure 11. Map produced from the GIS database showing the sinkhole area as a percentage of total area for each section in the study area.

apportionment of sinkholes which overlapped multiple sections, by the “square pond” problem, and by the slight discrepancies of section line locations. Additional sources of error could include errors in the hand-counts, digitizing errors in the original production of the DLG layers, undetected GIS procedural errors, or disparity in data sources. Despite sinkhole count differences present at the section level, the two overall study area counts were virtually identical. Therefore, we concluded that reliable sinkhole counts can be obtained using GIS-based methods.

In addition to producing accurate sinkhole counts, expanded statistical and spatial analyses are possible using GIS techniques. Descriptive statistics and figures can be easily generated for parameters such as sum of sinkhole area per section, sinkhole counts by section, and percent study area in sinkholes. For example, analysis of the percentage of sinkhole area per section (Fig. 11), as well as sinkhole counts per section (Fig. 12), can reveal sinkhole distribution trends that are useful for determining areas of greater risk for karst-related groundwater contamination and subsidence. The sinkhole database prepared in this study was used extensively by Panno *et al.* (in press) to generate a 1:24,000-scale sinkhole map of the Renault 7.5-minute Quadrangle. Digital geospatial data also provide long-term benefits for dynamic karst studies because new themes can be added, old themes deleted, and additional analyses and studies performed as new ideas are developed.

Finally, an examination of the time required to implement both methods revealed that the development and refinement of the GIS methodology for this investigation was approximately three times greater than the time consumed in hand-counting a single quadrangle. This was expected, but not discouraging, as the initial time and effort spent creating the database will facilitate quicker processing and broaden analysis opportunities for the study of additional quadrangles. With an established data-

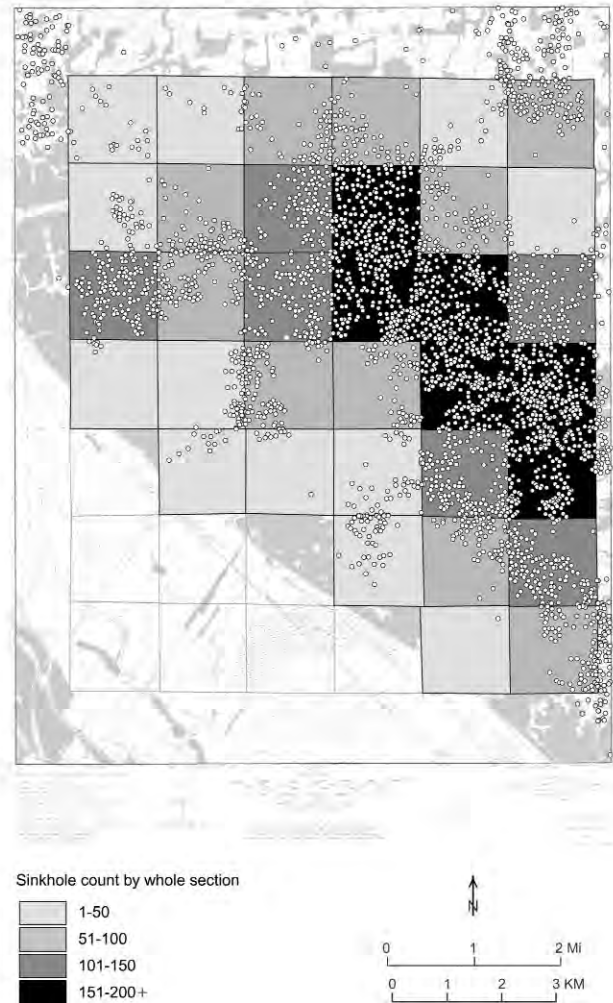


Figure 12. Map produced from the GIS database showing the number of sinkholes for each section in the study area. Map is layered with the Renault Quadrangle DRG, sinkhole count per section, and the sinkhole label points (each label point represents a countable sinkhole).

base in place, we expect that the processing of additional quadrangles with similar sinkhole density would require approximately 6-8 hours. Hand counting a densely populated quadrangle requires approximately 10-12 hours. Significant time savings would be realized when applying the GIS method to an area larger than a single quadrangle (e.g., the entire sinkhole plain). Finally, changes and revisions to GIS-produced maps and statistical data can be easily implemented, whereas changes to paper maps generally require the production of an entirely new, updated map.

CONCLUSION

Density and distribution studies of sinkholes in karst areas provide a means for identifying areas at risk for karst-related groundwater contamination and subsidence. The alternative of manually gathering and analyzing data on sinkhole density and distribution in mature karst terranes is a tedious and time-consuming process.

Differences between the sinkhole counts derived from manual and GIS-based methods for our study area were statistically negligible. The GIS method employed in this investigation yielded accurate sinkhole counts, provided opportunities for broader data analysis, and created a database for future analyses. Although possible to complete by hand, the descriptive statistics and map figure relating to the percentage of sinkhole area per section would require significant time and effort to produce manually. The time required to develop the GIS method was approximately three times greater than the time required to complete the hand-count of sinkholes on the paper quadrangle map. However, once the method and database are in place, additional quadrangles can be processed in about one-half the time required for the manual method.

ACKNOWLEDGEMENTS

The authors thank Edward Mehnert, Beverly Herzog, Robert Krumm, and Jonathan Goodwin for their critical review of this document and for their suggestions that greatly improved the quality of this document. This research was supported by the Illinois State Geological Survey, Illinois Department of Natural Resources. Publication of this article has been authorized by the Chief of the Illinois State Geological Survey.

REFERENCES

- Aley, T., Moss, P., & Aley, C., 2000, Delineation of recharge areas for four biologically significant cave systems in Monroe and St. Clair counties, Illinois: Unpublished final report to the Illinois Nature Preserves Commission and the Monroe County Soil and Water Conservation District, 254p.
- Applegate, P., 2003, Detection of sinkholes developed on shaly Ordovician limestones, Hamilton County, Ohio, using digital topographic data: dependence of topographic expression of sinkholes on scale, contour interval, and slope: *Journal of Cave and Karst Studies*, v. 65, n. 2, p. 126-129.
- Brezinski, D.K., & Dunne, L.E., 2001, Geographic Information Systems (GIS) applications to karst studies - Frederick Valley, Maryland: [Extended Abstract] in *Digital Mapping Techniques '01 - Workshop Proceedings*, U.S. Geological Survey Open-File Report 01-223, Tuscaloosa, Alabama, May 20-23, 2001, p. 207-208.
- Cote, W.E., 1972, Guide to the use of Illinois topographic maps: Illinois State Geological Survey Educational Extension Service Publication (revised 1978), Killey, M.M., DuMontelle, P.B., and Reinertsen, D.L., p. 9.
- Denizman, C., & Randazzo, A.F., 2000, Post-Miocene subtropical karst evolution, lower Suwannee River basin, Florida: *Geological Society of America Bulletin*, v. 112, n. 12, p. 1804-1813.
- Ford, D.C., & Williams, P.W., 1992, *Karst Geomorphology and Hydrology*: New York, Chapman and Hall, 601 p.
- Green, J.A., Marken, W.J., Alexander, E.C., & Alexander, S.C., 2002, Karst unit mapping using geographic information system technology, Mower County, Minnesota, USA: *Environmental Geology*, v. 42, n. 5, p. 457-461.
- Hyatt, J.A., & Jacobs, P.M., 1996, Distribution and morphology of sinkholes triggered by flooding following Tropical Storm Alberto at Albany, Georgia, USA: *Geomorphology*, v. 17, p. 305-316.
- Kochanov, W.E., 1999, The integration of sinkhole data and Geographic Information Systems: An application using ArcView 3.1: [Extended Abstract] in *Digital Mapping Techniques '99 - Workshop proceedings*, U.S. Geological Survey Open-File Report, Reston, VA, 1999, p.183.
- Panno, S.V., Weibel, C.P., Krapac, I.G., & Stormont, E.C., 1997a, Bacterial contamination of groundwater from private septic systems, in *Proceedings, Sixth Multidisciplinary Conference on Sinkholes and the Engineering and Environmental Impacts of Karst*, Springfield, MO, p. 1-7.
- Panno, S.V., Weibel, C.P., & Li, W.B., 1997b, Karst regions of Illinois: Illinois State Geological Survey Open File Report, 1997-2, 42 p.
- Panno, S.V., & Weibel, C.P., 1999, Delineation and characterization of the groundwater basins of four cave systems of southwestern Illinois' sinkhole plain: [Abstract] in *Karst Modeling: Symposium Proceedings*, A.N. Palmer, M.V. Palmer & I.D. Sasowsky (eds.), Karst Waters Institute Special Publication 5, Charlottesville, VA, p. 244.
- Panno, S.V., Hackley, K.C., Hwang, H.H., & Kelly, W.R., 2001, Determination of the sources of nitrate contamination in karst springs using isotopic and chemical indicators: *Chemical Geology*, v. 179, p. 115.
- Panno, S.V., Kelly, W.R., Weibel, C.P., Krapac, I.G., & Sargent, S.L., 2003, Water Quality and Agrichemical Loading in Two Groundwater Basins of Illinois' Sinkhole Plain: Illinois State Geological Survey Environmental Geology Series 156, 36p.
- Panno, S.V., Angel, J.C., Nelson, D.O., Weibel, C.P., & Devera, J.A., 2004, Distribution and Density of Sinkholes: Renault 7.5 Minute Quadrangle: Illinois State Geological Survey Quadrangle Series Map, (in press).
- Snedecor, G.W., & Cochran, W.G., 1989, *Statistical methods*: Ames, Iowa State University Press, 503 p.
- Szukalski, B.W., 2002, Introduction to cave and karst GIS: *Journal of Cave and Karst Studies*, Cave and Karst Studies Special Issue, v. 64, n. 1, p. 3.
- U.S. Census Bureau, 2000, State and County quickfacts, <http://quickfacts.census.gov/qfd/index.html>.
- U.S. Geological Survey (USGS), 1993a, Renault, IL: U.S. Geological Survey 7.5 minute quadrangle map, 1:24,000 scale, 1 sheet, mapped 1968, revised 1993, Denver, CO.
- U.S. Geological Survey (USGS), 1993b, Renault, IL: U.S. Geological Survey hypsography DLG map, 1:24,000 scale, 1 sheet, mapped 1970, revised 1993.
- U.S. Geological Survey (USGS), 1993c, Renault, IL: U.S. Geological Survey hydrography DLG map, 1:24,000 scale, 1 sheet, mapped 1970, revised 1993.
- Waite, L.A. & Thomson, K.C., 1993, Development, Description, and Application of a Geographic Information System Data Base for Water Resources in Karst Terrane in Greene County, Missouri: Rolla, Missouri, U.S. Geological Survey Water-Resources Investigations Report 93-4154, 31p.
- White, W.B., 1988, *Geomorphology and Hydrology of Karst Terranes*: New York, Oxford University press, 464 p.
- Willman, H.B., Atherton, E., Buschbach, T.C., Collinson, C., Frye, J.C., Hopkins, M.E., Lineback, J.A., & Simon, J.A., 1975, *Handbook of Illinois Stratigraphy*, Urbana, Illinois: Illinois State Geological Survey, Bulletin 95, 261p.

STYGOBITES ARE MORE WIDE-RANGING THAN TROGLOBITES

JOHN LAMOREUX

Department of Environmental Sciences, University of Virginia, Clark Hall, 291 McCormick Rd., P.O. Box 400123, Charlottesville, VA 22904-4123 USA lamoreux@virginia.edu

Stygobites are thought to be wider ranging than troglobites in the contiguous 48 United States. This assumption is confirmed by showing that stygobite species are recorded from more counties than troglobite species (Mann Whitney $U = 80189$, $Z = -6.781$, $P < 0.0001$). The properties of water flow through caves may allow greater dispersal opportunities for stygobites above the normal water table during floods and could be one reason for the larger ranges of these species.

Christman and Culver (2001) assume that stygobites, aquatic cave-dwellers, are wider ranging than their terrestrial counterparts, troglobites. Similarly, Culver *et al.* (2000) state that troglobites are confronted with different extinction risks than stygobites, because they generally have smaller range sizes. However, the assumption that troglobites have smaller range sizes is not based on data provided by Christman and Culver (2001) or Culver *et al.* (2000), nor related articles (Culver 1999; Culver *et al.* 1999; Culver *et al.* 2003). The percentage of troglobites endemic to a county in the United States is greater than for stygobites (Culver *et al.* 2000). However, this fact alone does not mean that stygobites are generally wider ranging because Culver *et al.*'s (2000) analysis does not consider range sizes of non-endemic species. Christman and Culver (2001) list the median number of counties in which both groups of cave fauna are present as three, which when taken alone, indicates a lack of range size difference between the two groups.

Using the Karst Waters Institute data from the web (<http://www.karstwaters.org> viewed online 4/27/03), I counted the number of counties in which each stygobite and troglobite species and subspecies was present in order to test whether stygobites were more widespread. I excluded interstitial species (listed as A1 species in the dataset, $N = 47$) from this analysis because they are poorly studied (this leaves 298 stygobites and 708 troglobites distributed across 538 counties). Because the distribution of stygobites and troglobites per county is similar to the range size distributions of most other organisms in being skewed right (Gaston 1998) (skewness statistic after log transformation = 1.67), I employed non-parametric Mann-Whitney U test. Stygobite species occur in more counties than troglobites (Stygobite Mean = 4, Std. Error = 0, $N = 298$, Range = 44; Troglobite Mean = 3, Std. Error = 0, $N = 708$, Range = 82; overall Mann Whitney $U = 80189$, $Z = -6.781$, $P < 0.0001$). The number of counties in which a cave-limited species is present should approximate the relative range size of that species. This analysis confirms earlier assumptions (Christman & Culver 2001; Culver *et al.* 2000) that stygobites are more wide-ranging than troglobites.

The data set used in this study contains potential biases (Christman & Culver 2001; Culver *et al.* 2000), two of which are particularly relevant to the present study: differences in our knowledge of aquatic and terrestrial taxa, and variations in county size. Certain aquatic groups have not been subject to the same level of taxonomic rigor as troglobites. However, Culver *et al.* (2000) note that the percentages of major cavernicole groups are similar to those of other well-studied temperate regions (Juberthie & Decu 1994). Furthermore, the number of species described since 1960 and the number of range extensions (as measured by additional county records) is nearly equivalent for stygobites and troglobites (Culver *et al.* 2000). One clear problem noted by Culver *et al.* (2000) involves the Edwards Aquifer (Texas), which extends under multiple counties but can only be accessed at a single spring. However, if access to this aquifer were possible in all counties, it would only reinforce the present findings by extending the known ranges of stygobites.

Similarly, Christman and Culver (2001) demonstrate that there is no correlation between the size of county and number of cave species across the US as a whole. Florida and Texas counties that contain cave species are larger than their counterparts in other states (mean area of FL and TX counties = 1837 km², $N = 65$; mean of the rest of counties = 1467 km², $N = 569$) (county area data from ERSI 2000), though the difference is not significant ($df = 632$, t statistic = -1.117, $P = 0.264$). This is important because the Florida and Texas counties contain more stygobites relative to troglobites than any other region of the country (Culver *et al.* 2003). Not only are stygobites found in more counties than troglobites in these states, the counties tend to be larger as well. Because the analysis relies on number of counties in which each species is present to reflect relative range size, the difference between the range sizes of stygobites and troglobites is likely under-represented.

Several possibilities have been put forward about why stygobites are more widespread than troglobites. Holsinger (2000) notes the tiny size of some stygobites as a trait that allows them to be unusually good dispersers. While discussing the larger numbers of endemic troglobites, Culver *et al.* (2000)

suggest that the greater degree of aquatic habitat “in the vertical extent” of caves probably indicates more connectivity between aquatic habitats in caves. Similarly, Christman and Culver (2001) state that there are more connections between aquatic habitats because caves form at or below the water table.

The climate of most caves is exceptionally stable (Poulson & White 1969). One aspect of the subterranean environment that does change is the variation in water volume, especially during floods. Unlike above ground streams, cave streams cannot overflow their banks and release flood waters across a floodplain. Instead, caves have relatively extreme increases in water depth during major flood events (White *et al.* 1995). During high water periods flooded passages should allow aquatic dispersal, while there may be no equivalent opportunity for terrestrial species to disperse. This simple characterization of added opportunities for dispersal is no different than earlier statements about the aquatic habitat being greater in extent, but it raises the possibility that the dispersal advantage stygobites have over troglobites might extend above the normal water table.

ACKNOWLEDGMENTS

I am grateful to the Karst Waters Institute for making their data freely available. I thank David Culver for his comments on a draft manuscript and for encouraging me to publish. I thank Meghan McKnight for her comments, Wes Sechrest for his help with statistics, and Alan Howard for the initial impetus to write the article.

REFERENCES

- Christman, M.C., & Culver, D.C., 2001, The relationship between cave biodiversity and available habitat: *Journal of Biogeography*, v. 28, p. 367-380.
- Culver, D.C., 1999, Ecosystem and species diversity beneath our feet, *in* Ricketts, T.H., Dinerstein, E., Olson, D.M., Loucks, C.J., Eichbaum, W., DellaSala, D., Kavanagh, K., Hedao, P., Hurley, P.T., Carney, K.M., Abell, R., & Walters, S., (eds.), *Terrestrial Ecoregions of North America: A Conservation Assessment*: Washington, D.C., Island Press, p. 56-59.
- Culver, D.C., Christman, M.C., Elliott, W.R., Hobbs III, H.H., & Reddell, J.R., 2003, The North American obligate cave fauna: Regional patterns: *Biodiversity and Conservation*, v. 12, p. 441-468.
- Culver, D.C., Hobbs III, H.H., Christman, M.C., & Master, L.L., 1999, Distribution map of caves and cave animals in the United States: *Journal of Cave and Karst Studies*, v. 61, no. 3, p. 139-140.
- Culver, D.C., Master, L.L., Christman, M.C., & Hobbs III, H.H., 2000, Obligate cave fauna of the 48 contiguous United States: *Conservation Biology*, v. 14, no. 2, p. 386-401.
- Environmental Systems Research Institute (ESRI), 2000, Data and maps CD-ROM for ArcView: Redlands, California, ESRI.
- Gaston, K.J., 1998, Species-range size distributions: products of speciation, extinction and transformation: *Philosophical Transactions of the Royal Society, London, Series B., Biological Sciences*, v. 353, no. 1366, p. 219-230.
- Holsinger, J.R., 2000, Ecological derivation, colonization, and speciation, *in* Wilkens, H., Culver, D.C., & Humphreys, W.F., (eds.), *Ecosystems of the World 30: Subterranean Ecosystems*: Amsterdam, Netherlands, Elsevier Science, p. 399-415.
- Juberthie, C., & Decu, V., (eds.), 1994, *Encyclopedia Biospeologia: Moulis, France*, Societe de Biospeologie.
- Poulson, T.L., & White, W.B., 1969, The cave environment: *Science*, v. 165, no. 3897, p. 971-981.
- White, W.B., Culver, D.C., Herman, J.S., Kane, T.C., & Mylroie, J.E., 1995, Karst lands: *American Scientist*, v. 83, p. 450-459.

HOLOCENE CLIMATIC VARIATION RECORDED IN A SPELEOTHEM FROM MCFAIL'S CAVE, NEW YORK

PHILIP E. VAN BEYNEN¹, HENRY P. SCHWARCZ², AND DEREK C. FORD²

¹ Department of Environmental Science and Policy, SCA 238, University of South Florida, Tampa, FL 33620, USA

² School of Geography and Geology, McMaster University, Hamilton Ontario L8S 4K1, CANADA

A speleothem collected from McFail's Cave, central New York, was analyzed in order to produce a high resolution paleoclimatic record for this region. The record is dated by Th/U ICP Mass Spectrometry. Variation in growth rates and $\delta^{18}\text{O}$ values for the period 0 to 7.6 ka revealed three distinct intervals: maximum warmth and wettest from 7.6 to 7.0 ka; a slow steady cooling from 7.0 to 2.5 ka; and fairly constant temperatures for the last few thousand years. The climatic optimum appears to have occurred at or before 7.6 ka. These changes are in agreement with regional stable isotopic and lake level records from the Finger Lakes in NY, suggesting the climatic changes are regional in scope. Enrichment of ^{18}O in speleothems deposited at this time suggests that temperatures could potentially have been 5°C warmer than at present, which is consistent with pollen records for this region. However, a northward shift in the Jet Stream during the period would have affected the source area of the rainfall, providing heavier $\delta^{18}\text{O}$ values, an effect that would potentially reduce our temperature increase of 5°C. Quantification of this shift's contribution to the temperature increase recorded by our speleothem is extremely difficult due to the lack of information about the exact location of the Jet Stream. $\delta^{13}\text{C}$ values are generally uniform but show a brief vegetational optimum at ~7.5 ka and increased density from 5.5 to 2.5 ka, suggesting a wetter climate.

Calcite speleothems precipitated in caves have been shown to record paleo-environmental change through the Late Quaternary and Holocene periods (Harmon *et al.* 1978; Gascoyne 1992; Bar-Matthews *et al.* 1999). Stable isotopic analysis of microgram samples of calcite and their fluid inclusions, coupled with accurate U/Th dating techniques, may provide high-resolution records of the climate and vegetation changes above a cave (Schwarcz 1986). Paleoclimatic inferences may be drawn by measuring growth rates of millennial (Hennig *et al.* 1983) to annual scale (Broecker *et al.* 1960; Baker *et al.* 1993; Shopov *et al.* 1994; 1997; Genty & Quinif 1996; Roberts *et al.* 1998; van Beynen 1998; Lauritzen *et al.* 1999; Perrette *et al.* 1999).

As water from rain and snow melt percolates through the soil, it absorbs soil CO_2 produced by root respiration, increasing its acidity. On reaching limestone bedrock beneath, the acidic water dissolves calcium carbonate until thermodynamic equilibrium with the ambient partial pressure of CO_2 (P_{CO_2}) is attained (Plummer *et al.* 1979). On entering an airfilled cave, the CO_2 may degas rapidly because P_{CO_2} is usually lower than in the soil and tiny fissures above it; precipitation of part of the dissolved CaCO_3 then results (Plummer *et al.* 1979). Where calcite has formed in oxygen isotopic equilibrium with ambient water, the isotopic fractionation between calcite and water, $\Delta_{\text{c-w}}$, is dependent on the temperature (O'Neill *et al.* 1975):

$$1000 \ln \Delta_{\text{c-w}} = 2.78 \times 10^6 T^{-2} (\text{K}^{-2}) - 2.89 \quad [1]$$

Where $\Delta_{\text{c-w}} = (1000 + \delta^{18}\text{O}_{\text{c}}) / (1000 + \delta^{18}\text{O}_{\text{w}})$ and $\delta^{18}\text{O}_{\text{c}}$ and $\delta^{18}\text{O}_{\text{w}}$ are the $\delta^{18}\text{O}$ values of calcite and water, respectively and

K is the equilibrium constant. We can test for equilibrium deposition by analysis of multiple samples taken from a single growth layer. Equilibrium deposits display the following characteristics: a) there is no variation in $\delta^{18}\text{O}$ along the growth layer; b) there is no correlation between $\delta^{18}\text{O}$ and $\delta^{13}\text{C}$ (Hendy & Wilson 1968). Deep interior cave temperatures are usually invariant over the year and close to the mean annual surface temperature above the cave (Wigley & Brown 1976). The oxygen isotope records of speleothems may therefore offer proxy records of paleotemperatures and climate change (Schwarcz 1986). In practice, however, it is difficult to use analysis of speleothems to determine the temperature of deposition (T) because the relation between T and $\delta^{18}\text{O}_{\text{c}}$ is principally controlled by two factors which have opposing T -dependencies: the isotopic fractionation between calcite and water decreases with increasing T by about 0.24 ‰/°C; but $\delta^{18}\text{O}$ (ppt), the isotopic composition of the meteoric precipitation, increases with increasing T by between 0.3 and 0.7 ‰/°C, a rate which varies locally and with time as a consequence of differing sources and storm tracks (Schwarcz 1986). The balance between these factors (as well as others, discussed in Schwarcz 1986) may be such that the T -dependence of $\delta^{18}\text{O}_{\text{c}}$ ($\gamma = d \delta^{18}\text{O}_{\text{c}}/dT$) may vary in magnitude and sign from one site to another. In general we expect that at a given locality the sign of γ will remain the same through time (Frumkin *et al.* 1999).

It is possible in theory to determine T directly by simultaneous analysis of the calcite and of water trapped as fluid inclusions in it (Schwarcz *et al.* 1976). It is also useful to use $\delta^{18}\text{O}_{\text{c}}$ by itself as a proxy record of climate. To do so we must,

Please send correspondence to Dr. Philip van Beynen: vanbeyne@cas.usf.edu.

however, determine the sign of γ within the speleothem in question. We may do this by comparison of $\delta^{18}\text{O}$ of modern calcite with that of Ice Age speleothems that are inferred to have formed at lower temperatures. Similarly, for post-Ice Age deposits (the Holocene—the last 11,000 years), we can assume that deposits dating to a well established mid-Holocene warm phase (the Hypsithermal) were deposited at warmer temperatures than modern calcite. The gradient in $\delta^{18}\text{O}$ between calcite formed in these differing periods defines the sign of γ .

The $\delta^{13}\text{C}$ record in speleothems is a function of the vegetation density and types of plants growing above the cave. The proportion of dissolved inorganic carbon in recharge water derived from plant respiration increases with plant density and plant biological activity. $^{13}\text{C}/^{12}\text{C}$ ratios in speleothems represent a mixture of carbon-derived soil CO_2 and of the limestone bedrock (~0‰). Drip rates, length of flow path, and rates of outgassing and calcite precipitation may also affect the $\delta^{13}\text{C}$ signal (Wigley *et al.* 1978). Where $\delta^{13}\text{C}$ of plants has remained constant, lower $\delta^{13}\text{C}$ (lighter) values indicate more forested environments and/or greater respiratory activity in warmer, wetter conditions compared to the higher $\delta^{13}\text{C}$ (heavier) values beneath more open, less humid vegetative environments. Frumkin *et al.* (1999), in a study of speleothems from Nahal Qanah Cave, Israel, showed that more depleted $\delta^{13}\text{C}$ values in a Holocene speleothem correlated with increased density of vegetation there.

Most previous research on the paleoclimate of the Holocene epoch in the northeastern USA has produced fairly broad interpretations often with only brief snapshots in time. The dates used in these below papers were originally radiocarbon dates, but as our Th/U dating is in calendar years, we have converted the original dates of the articles into calendar years using the INTCAL98 conversion data from Stuiver *et al.* (1998). This allows direct comparison between our data and that from the below studies. Prentice *et al.* (1991) gave 3000-year increments for the Holocene using pollen data. They concluded that the climate at 6.9 to 10.2 ka (ka = thousand years) was warmer and wetter than present, and that after 3.5 ka BP (BP – before present) summer temperatures declined. From studies of past distributions of tree species, Davis *et al.* (1980) concluded that this region was warmer before 5.7 ka. Jackson and Whitehead (1991) highlighted three periods from their pollen records; a) 10.2 to 5.7 ka: summer temperatures 1.0 to 1.6°C higher than present; b) 5.7 to 3.5 ka: transition to more modern forest assemblages; and c) after 3.5 ka: modern vegetation present. Lacustrine sediments from the Finger Lakes Region of New York show high lake levels at ~6.3 to 9.5 ka with maximum levels at 7.8 ka (Dywer *et al.* 1996). Studies of Cayuga Lake, NY, sediments show a warm period centered on ~8.9 ka (Anderson *et al.* 1997); and high CaCO_3 accumulation rates (Mullins 1998). Therefore, there is some debate as to the precise timing of the Hypsithermal in this region, with estimates ranging between 7.8 ka and 8.9 ka BP.

In this paper we have used stable oxygen and carbon isotopic records from a speleothem collected from McFail's Cave,

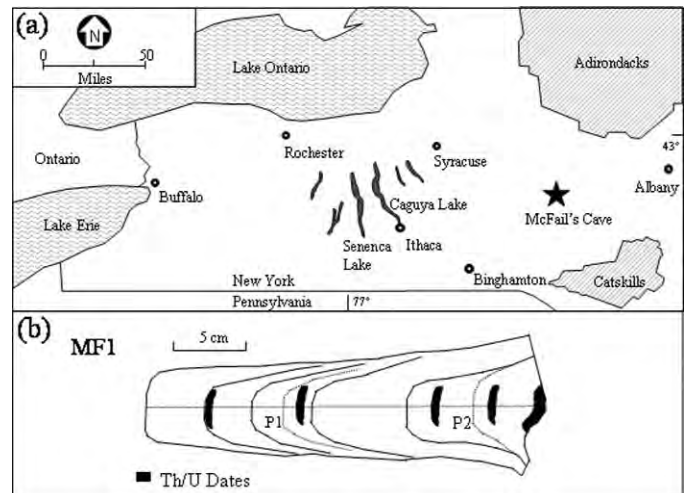


Figure 1. a) Location of McFail's Cave; b) sampling sites for dating; straight dotted line running up the middle of the sample shows the transect taken for stable isotope analysis. P1 and P2 show positions of stable isotope profiles taken for testing for equilibrium (see text).

New York to establish the most detailed isotopic record for the northeastern USA to date. We will also determine how our Holocene climate record for the NY region compares to other proxy records for the area.

STUDY AREA

McFail's Cave is located 3 km northeast of Cobleskill (38°22'N, 90°39'W) in Schoharie County, New York (Fig. 1). The sample was obtained from an active river passage that is traceable for 4.5 km at an elevation of 400 to 430 m asl. It is developed in limestone and dolostone beds of the Helderberg Group (Upper Silurian-Lower Devonian) ranging up to 50 m in thickness, and covered by up to 100 m of younger limestones (Palmer, 1975). The average thickness of bedrock above the cave is between 50-70 m.

The region was glaciated during the late Wisconsin, when 50 m of glacial till was deposited in the Cobleskill Valley (Palmer 1975). However, there is only a thin veneer of till above the cave. The vegetation cover includes a small marsh and some fields surrounded by a closed canopy Carolinian forest. The marsh is fed by groundwater from surrounding hill-sides and is the source for much of the cave dripwater. The regional climate is temperate with mean monthly temperatures ranging from -4.7°C in January to 19.1°C in July (climatic data from National Climatic Data Center, 2003). The average cave temperature for the year is 7.3°C (A. Palmer pers. comm.). The mean total precipitation is 960 mm and is rather uniformly distributed over the year (NCDC, 2003).

The vegetation above McFail's Cave is dominated by C_3 plants (forest environment as opposed to C_4 plants which are predominately grasses) that normally display $\delta^{13}\text{C}$ values averaging around -26‰ (Deines 1980). Pollen studies from this

Table 1. U-series dates for MF1.

mm from Base	U (ppm)	$^{234}\text{U}/^{238}\text{U}$	$^{230}\text{Th}/^{234}\text{U}$	$^{230}\text{Th}/^{232}\text{Th}$	Uncorrected Age (ka)	Corrected Age (ka)
2	1.63	2.194 ± 0.0021	0.069 ± 0.0004	51.26 ± 0.37	7.826 ± 0.047	7.606 ± 0.047
37	1.61	2.244 ± 0.0021	0.068 ± 0.0004	306.76 ± 2.60	7.606 ± 0.057	7.570 ± 0.057
75	1.24	2.250 ± 0.0019	0.066 ± 0.0006	105.58 ± 1.15	7.425 ± 0.077	7.324 ± 0.077
165	0.77	2.256 ± 0.0029	0.046 ± 0.0006	23.35 ± 0.33	5.126 ± 0.072	4.805 ± 0.072
225	1.63	2.317 ± 0.0020	0.022 ± 0.0019	15.42 ± 1.31	2.484 ± 0.214	2.245 ± 0.214

region indicate that past vegetation at this site was also dominantly C_3 (Jackson & Whitehead 1991).

METHODS

SAMPLE COLLECTION

Speleothem MF1 is a stalagmite collected from the downstream end of McFail's Cave. It was previously found to be of Holocene age through U-series dating using alpha spectrometry (Gascoyne 1979). The stalagmite was cut along its growth axis and polished to provide a cross section. Micro-samples of 0.1 mg were drilled (high speed dental drill) along growth layers to test for equilibrium deposition and up the growth axis, providing 136 samples for oxygen and carbon analysis. Calcite samples of 1.0–1.25 g each were taken from the speleothem for Th/U dating as illustrated in Figure 1. Calcite samples for Th/U dating were taken within defined growth layers to maximize the resolution of the dates.

U-SERIES DATING

U-series dating was undertaken using inductively coupled plasma (ICP) mass spectrometry. U and Th were extracted from the calcite samples in a clean lab in McMaster University using the methods of Li *et al.* (1989). The $^{229}\text{Th}/^{236}\text{U}$ spike was calibrated by J. Lundberg, Carleton University. The Th and U extracts were analyzed by A. Simonetti on a VG IsoProbe multicollector ICP mass spectrometer at the Center for Research in Geochemistry and Geodynamics (GEOTOP), University of Quebec at Montreal, using the following protocol.

Samples were analyzed in static multicollection mode using four Faraday collectors (high mass side). Typical settings for the ICP source are the following: Forward power- 1350 watts; Cool gas- 13.50 L/min. (Ar); Intermediate gas- 1.030 L/min. (Ar); Nebulising gas- 0.8–0.9 L/min. (Ar). The instrument settings were optimized using an ICP-MS-grade uranium solution. Samples were conditioned in 2% HNO_3 and introduced into the ICP source using an Aridus© microconcentric nebuliser at an uptake rate of $\sim 50 \mu\text{l}/\text{min}$ (verified periodically). The sweep gas settings for the Aridus© introduction system typically varied between 3.5–4.0 L/min argon and 10–15 ml/min nitrogen. Oxide levels are systematically verified and are typically <1% of the uranium metal signal. Data acquisition consisted of a 50 seconds "on-peak-zero" measurement (gas and acid blank) prior to aspiration of the sample. Upon aspiration of the sample, two half-mass unit baseline measure-

ments were conducted (15 seconds each) within the mass range of data acquisition (232.5 to 236.5). Isotope ratios were measured for 50 scans at 10 seconds integration time. Subsequent to each analysis, washout consisted of using both 4% and 2% HNO_3 wash and rinse solutions, respectively for a combined 10–15 minutes.

The acquisition of Th isotopic measurements is essentially identical to that for uranium with the exception that data acquisition consisted of 60 scans at 5 seconds integration time, and three Faraday collectors (instead of four) were used. In addition, washout times were slightly longer at approximately 20 minutes. Data reduction was carried out using software developed by B. Ghaleb.

STABLE ISOTOPE ANALYSIS

$\delta^{18}\text{O}$ and $\delta^{13}\text{C}$ of calcite were measured on a VG Sira II mass spectrometer in an Autocarb automated carbonate analyzer at McMaster University. Isotopic ratios are reported with respect to the VPDB standard in per mil units (‰). NBS-19 is the laboratory reference standard used in this study. The precision of analyses for both isotopes is $\pm 0.1\%$.

RESULTS

U-SERIES DATES

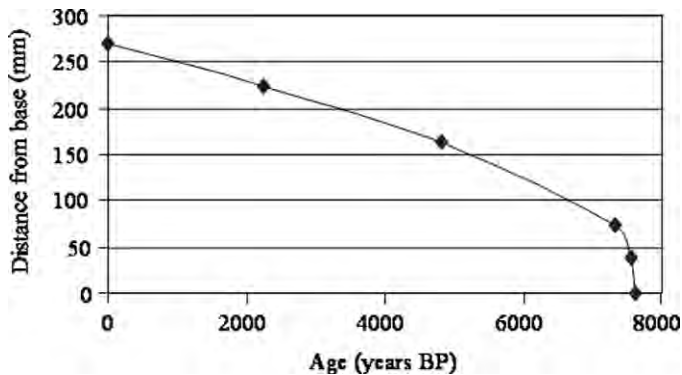
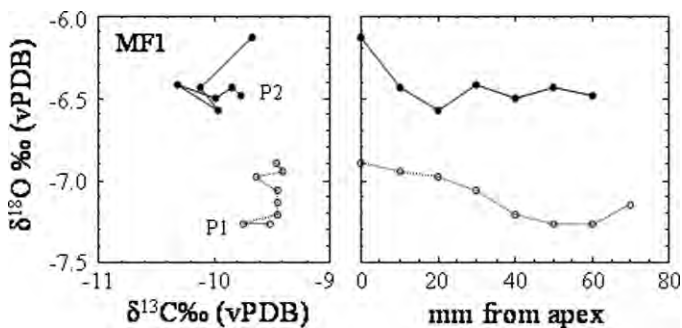
Results of the U-series dating are presented in Table 1. Measured U concentrations are similar in all samples and high enough to permit precise estimates. Errors for the U/Th ages are reported to two standard deviations. $^{234}\text{U}/^{238}\text{U}$ ratios are also similar, suggesting that the source environment is stable. All of the Th/U ages obtained are in their correct stratigraphic order.

THE GROWTH RATES OF THE STALAGMITE

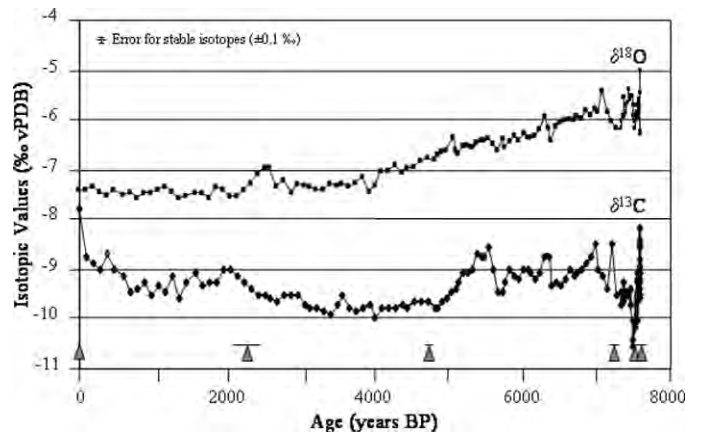
Annual growth rates were calculated by dividing the portion of calcite (mm) by the number of years that portion was deposited over (derived from Th/U dates). The calculated annual growth rates between dated sections of MF1 may provide insight into any environmental changes above the cave (Table 2 and Fig. 2). The faster the growth rate, the warmer and/or wetter the climate is above the cave (Hennig 1983; Dreybrodt 1982). We observe a distinct change in growth rate, from a maximum value near the base of c. 1.0 mm/y to a rate two orders of magnitude lower through the remainder of the history of this stalagmite. These growth rates are within the

Table 2. Annual growth rates for MF1.

Distance from Base (mm)	Time of Growth (years)	Length of Calcite (mm)	Rate of Growth (mm/yr)
0-37	36	37	1.027
38-75	246	37	0.150
76-165	2519	89	0.035
166-225	2560	59	0.023
226-270	2245	44	0.019

**Figure 2. Variations in height with age, showing rapid deceleration of growth rates after the first 250 years.****Figure 3. Hendy tests for equilibrium deposition of MF1. Equilibrium deposition is generally assumed if the $\delta^{18}\text{O}$ range is less than 0.8‰. P1 and P2 are the profiles drilled along two growth rings within MF1.**

known range for speleothems from temperate climates (Baker *et al.* 1998; van Beynen 1998). Elsewhere, high growth rates have occurred during periods of temperature maxima and/or wetter conditions while growth declined during cooler/drier periods (Hennig *et al.* 1983; Railsback *et al.* 1994; Genty & Quinif 1996; Schwehr 1998; Brook *et al.* 1999; Qui *et al.* 1999). As the earlier part of the Holocene is known to have been warmer than present in the nearby Finger Lakes Region, NY (Mullins 1998), we might expect higher growth rates near the base of MF1. For the first 40 years of growth, the rates are very high, > 1 mm per year. The next 250 years also have fast growth though an order of magnitude lower. Overall, 25% of the speleothem was deposited during approximately its first 300 years, the rest over the remaining 7300 years. Such rapid growth from 7.6 to 7.3 ka for MF1 is consistent with the

**Figure 4. $\delta^{18}\text{O}$ and $\delta^{13}\text{C}$ values for MF1.**

warm/wet period from 10.2 to 6.9 ky reported by Prentice *et al.* (1991) and Jackson and Whitehead (1991). Pielou (1991) places the Holocene Hypsithermal at ~7.8 ka in central New York, which is the same period that Dywer *et al.* (1996) and Mullins (1998) found high water levels at Finger Lakes of NY. These studies suggest MF1 was responding to a warm and wet climate in the NY region during this time.

STABLE ISOTOPE ANALYSIS

a) Isotopic equilibrium test

To test whether the speleothem was deposited in isotopic equilibrium, profiles were drilled precisely along two of its growth layers. The criteria for equilibrium deposition are that there must be no correlation between the $\delta^{18}\text{O}$ and $\delta^{13}\text{C}$ for each profile or any variation in $\delta^{18}\text{O}$ greater than 0.8‰ (Hendy & Wilson 1968; Gascoyne 1992). Results shown in Figure 3 indicate that MF1 was deposited in equilibrium as both P1 and P2 in the left box obviously have no correlation between $\delta^{18}\text{O}$ and $\delta^{13}\text{C}$ (averaging at $r = 0.08$, significance = 0.29) and in the right hand box the profiles have $\delta^{18}\text{O}$ deviation < 0.8‰.

b) The $\delta^{18}\text{O}$ records

Figure 4 displays the $\delta^{18}\text{O}$ records for the MF1. Maximum $\delta^{18}\text{O}$ values are observed at the base of the stalagmite, during the period from 7.6 to 6.6 ka. $\delta^{18}\text{O}$ decreases gradually in a transition period from 6.6 to 2.2 ka and relatively stable values persist after that till present.

We know that the climate in this region around 10.2 to 6.9 ka BP was warmer than in the later Holocene. We may therefore infer that $\gamma > 0$ for this speleothem. Secondly, the trend of $\delta^{18}\text{O}$ values in MF1 during the Holocene shows that climate has been steadily cooling with only minor perturbations over the history of this deposit. The exceptionally high growth rates and $\delta^{18}\text{O}$ values at the base of the deposit suggest that growth began near the warmest phase of the Hypsithermal (Pielou 1991; Anderson *et al.* 1997).

(c) The $\delta^{13}\text{C}$ records

$\delta^{13}\text{C}$ values displayed in Figure 4 vary from -7.8 to

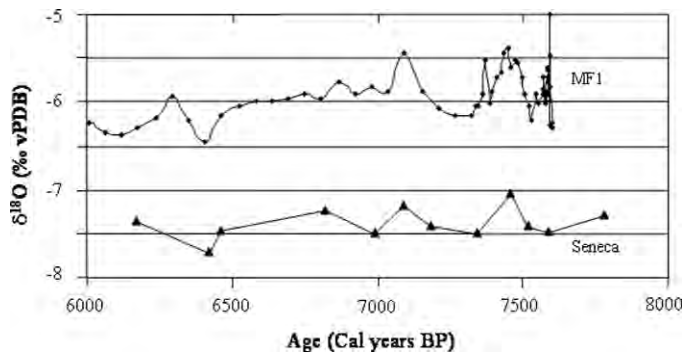


Figure 5. Comparison of MF1 $\delta^{18}\text{O}$ values with $\delta^{18}\text{O}$ values obtained from a marl record from Seneca Lake, NY (Anderson *et al.* 1997).

-10.8‰, a range of only 3 per mil. Dorale *et al.* (1998) show that for changes from C₃ to C₄ vegetation, shifts of 7‰ in $\delta^{13}\text{C}$ of speleothem calcite are required. What the McFail's $\delta^{13}\text{C}$ record shows is that forests (C₃ plants) have been the predominant vegetation above the cave with no evidence of grassland environments until very recently. Therefore, the $\delta^{13}\text{C}$ values record changes in the density of the forest above the cave. Prentice *et al.* (1991) showed that forest (C₃) existed in this region throughout the growth of this speleothem, with only tree composition changing (Jackson & Whitehead 1991). The dramatic decrease in the $\delta^{13}\text{C}$ values from 7.6 to 7.5 ka may mark the arrival of forest vegetation (*Carya*, *Ulmus*, *Fagus* and *Tsuga* species). The period from 7.0 to 5.5 with its heavier $\delta^{13}\text{C}$ values suggests a decline in the density of the forest, probably due to cooling of the regional climate. However, from 5.5 to 2.5 ka the $\delta^{13}\text{C}$ values lightened once more, even though temperatures continued to fall during most of this period. The only possible explanation for such a trend could be a wetter climate, generating more lush growth. The final 2.5 ka years show the $\delta^{13}\text{C}$ values trending towards heavier values, and as temperatures were relatively stable during this time, we suggest that climate became somewhat drier in the NY region. The steeper rise during the last 300 years may be associated with more intense deforestation by European populations (Foster & Zebryk 1993).

DISCUSSION

CLIMATE CHANGE INFERRED FROM CHANGES IN $\delta^{18}\text{O}_c$

Stalagmite MF1 appears to have begun its growth near the climatic high-point of the Holocene Hypsithermal as derived by Perliou (1991) and Anderson *et al.* (1997). This is principally suggested by the record of $\delta^{18}\text{O}$ but is also consistent with the history of the growth rate and slightly less clearly defined by the record of the $\delta^{13}\text{C}$. It appears that $\gamma > 0$ for this speleothem: if γ remained more or less constant throughout the Holocene, then we would see a record of almost linearly decreasing temperature for the first 4,500 years of deposition (until ~3.0 ka BP) followed by stable climate until present.

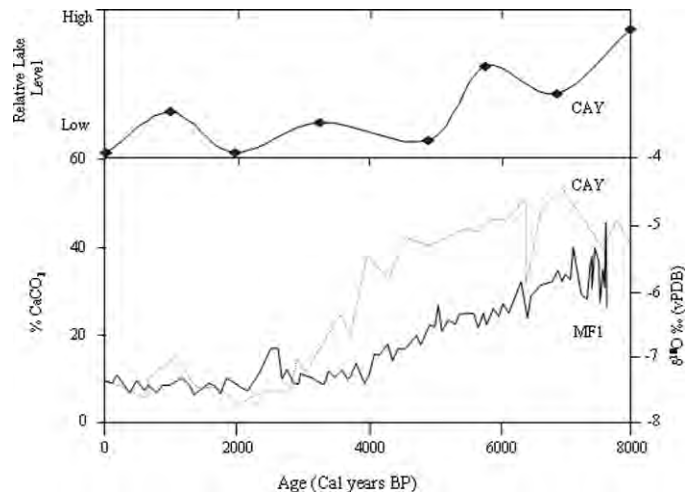


Figure 6. Comparison of MF1 $\delta^{18}\text{O}$ values with % CaCO_3 in sediment of Cayuga Lake and its relative lake levels (Mullins, 1998).

The climate during the period from 7.0 ka to 7.6 ka appears to be more variable than after this phase (Fig. 4). Two distinct peaks in $\delta^{18}\text{O}$ at 7.0 ka and 7.5 ka are separated by a prominent decline suggesting a short cooling. This cooling interval and the two warm periods delineating it are also found in the Seneca Lake $\delta^{18}\text{O}$ record (Anderson *et al.* 1997), thereby showing that the climate change recorded by MF1 was regional and not highly localized (Fig. 5). The Anderson *et al.* (1997) lake record shows the same trend of falling $\delta^{18}\text{O}$ values as the MF1 record. The decreasing trend in the $\delta^{18}\text{O}$ values in both records presumably represents falling temperatures.

The variability in the record during the aforementioned period is not apparent in the rest of the record. A possible explanation can be forwarded from the growth rates. This period had the fastest growth rates and because the speleothem was sampled at regular intervals, the sampling density would be the greatest for this section. The rest of the speleothem had slower deposition rates and consequently more years were averaged when each isotopic sample was taken, thereby removing some of the variability that was evident from 7.0 to 7.6 ka. However, we would stress that even if the sampling density was the same as for later in the record, the $\delta^{18}\text{O}$ isotopic values for this period would still have shown it to be the warmest part of the Holocene as measured by MF1.

Although we have shown similarity between our $\delta^{18}\text{O}$ record for McFail's Cave and a short record from Seneca Lake for the first 1600 years of MF1's growth, we must also investigate comparisons for the other 6000 years of its growth. On a regional scale the most complete record is Mullins' (1998) record of carbonate content of sediments (marl) deposited in Cayuga Lake, NY. Figure 6 shows the comparisons with: (a) inferred lake levels, where the author states that lower levels were analogous with drier/cooler conditions, and (b) marl concentrations in the lake sediment, where Mullins attributes higher carbonate content to higher summer temperatures. Both

these records show very similar trends to that of MF1, with warmer conditions in the earlier Holocene and a transition to cooler present climatic conditions by ~3.0 ka BP.

Most previous studies of the paleoclimate of the northeastern USA come from pollen records extracted from lake and bog sediments. Prentice *et al.* (1991) found that increased precipitation allowed hickory to expand in the Appalachian region 6.9 to 10.2 ka. Davis *et al.* (1980) noted that between 7.8 to 5.7 ka *Pinus*, *Strobus* and *Tsuga* were at higher elevations in the Adirondack and New England Mountains, suggesting temperatures warmer than present. MF1 does show this period as especially warm compared to the period before 7.0 ka. 5.7 to 3.5 ka saw the transition of Adirondack vegetation to more modern assemblages (Jackson & Whitehead 1991), a transition that is in accordance with the record of MF1. There was a retreat of hemlock after 3 ka that is indicative of decreasing summer temperatures (Prentice *et al.* 1991). Increasing *Picea* pollen after 2.5 ka also suggests decreasing temperatures (Jackson & Whitehead 1991). These two studies show that climate was cooler during the last 3000 years for the broader region around McFails Cave, which concurs with our $\delta^{18}\text{O}$ record.

TEMPERATURE OF CLIMATIC OPTIMUM FOR MF1

Dorale *et al.* 1992 calculated temperatures of deposition of speleothems from their $\delta^{18}\text{O}$ values using the following equation

$$\delta^{18}\text{O}_c = (0.695T + 986.4)\exp[2780/(273.15 + T)^2]^{-0.00289} - 1000 \quad [2]$$

where T is in °C. Using the present day annual average of 7.3 °C for Cobleskill, we obtain a present day $\delta^{18}\text{O}_c$ of 24.2‰ (SMOW) which is slightly higher than the observed value of 23.16‰. This discrepancy could be due to a difference in the T dependence of $\delta^{18}\text{O}$ (ppt) for the northeast of the USA compared with the north-central USA where Dorale *et al.* (1992) conducted their study. Rozanski *et al.* (1993) suggest a value of 0.58‰/°C rather than 0.695. Changing this value results in agreement between the calculated and observed present day $\delta^{18}\text{O}_c$ values. Using this revised equation it is possible to determine the temperature at McFail's Cave at the climatic optimum. Our average $\delta^{18}\text{O}_c$ value for c. 7.6 ka is 24.89‰ SMOW. Using the modified version of Equation [2] we obtain a temperature of 12.5°C, which would be ~5°C warmer than present day temperatures. We can compare this result with that of Prentice *et al.* (1991) who provide snapshots at 3 ka increments using isotherms inferred from pollen data for the northeastern USA to reconstruct January and July temperatures. Plotting our site on their maps for 6.9 ka BP, which is their warmest snapshot during the Holocene, we obtain a mean annual temperature of 11.8°C, which is 4.3°C warmer than present, in good agreement with our estimate.

Another factor that may have influenced the $\delta^{18}\text{O}$ of calcite through the Holocene is a change in the seasonal distribution of precipitation. Using weather records for nearby Cobleskill,

NY, we see that at present, precipitation is distributed approximately uniformly throughout the year. We also note that at present, the maximum range in temperature between winter and summer is about 28°C; assuming an isotopic temperature dependence of 0.58‰/°C, this represents a maximum W-S difference in $\delta^{18}\text{O}$ (ppt) of c. 16‰. More realistically, the difference in average winter and summer temperatures (October-March vs. April-September) is 9°C, which corresponds to a difference in $\delta^{18}\text{O}$ (ppt) of 5.2‰. For each 1% increase in the relative proportion of summer rain relative to winter snow + rain, we would increase $\delta^{18}\text{O}$ of average precipitation by 0.05‰. It is conceivable that there could have been as much as 10% more summer precipitation at the Hypsithermal due to retreat of the polar front (Dwyer *et al.* 1996) and decrease in winter storm activity. This could have accounted for an increase of about 0.5‰ in average annual precipitation which would be reflected in $\delta^{18}\text{O}$ of speleothem.

While the seasonal distribution of rainfall may have affected the $\delta^{18}\text{O}$ values of the speleothem, the source of the rainfall may also have changed. Evidence for such a change is provided by the interpretation of eolian deposits in the Central United States (Forman *et al.* 1995). As an explanation for arid conditions in their records in the mid-Holocene, the authors suggested that the Jet Stream had moved to higher latitudes, shifting the location of the Bermuda High which then funneled moisture to the Northeast and not the Mid-West. Around 3.0 ka BP the Jet Stream retreated southward, and consequently the Bermuda High channeled moisture from the Gulf of Mexico into the interior of the continent. McFail's Cave is located in this transitional zone of the Jet Stream, and therefore its movement may have changed the source of the rainfall that contributed to the seepage of the drip waters feeding MF1. However, this movement would also have affected the temperature of the air above and consequently within the cave as well. A Jet Stream to the north of the cave would have brought warmer temperatures and rainfall from a source area with heavier $\delta^{18}\text{O}$ values to McFail's Cave, while its retreat south would have had the opposite effect. The shifts in the location of the Jet Stream as identified by Forman *et al.* (1995) are recorded in our $\delta^{18}\text{O}$ data. However, the Forman article's aim was not to provide precise locations of the Jet Stream, and its exact position is not known throughout the Holocene. This makes quantification of the effect these shifts may have on our isotopic record nearly impossible. All that can be said with any confidence is that our estimate of temperature at 7.6 ka BP can be considered a maximum value.

CLIMATE CHANGE INFERRED FROM GROWTH RATE

Maximum growth rates for MF1 were from 7.3 to 7.6 ka. This is consistent with our $\delta^{18}\text{O}$ record, being indicative of warmer regional temperatures that would lead to faster growth rates (Dreybrodt 1982). However, the growth rates at the inception of deposition of this stalagmite are exceptionally high and suggest the occurrence of extraordinary climatic conditions at this time, possibly a combination of high tempera-

tures and high rainfall. A warm climate is shown in the higher lake levels at Cayuga Lake, NY (Mullins 1998) providing evidence for higher rainfall in this region during this period.

Another possibility could be the presence of denser forest cover, with greater respiration increasing the CO₂ dissolved in the percolation waters. Denser forest cover would be expected to lead to lower $\delta^{13}\text{C}$ values; such a trend is observed briefly around 7.5 ka BP.

CONCLUSIONS

The climatic interpretation derived from records of both $\delta^{18}\text{O}$ and speleothem deposition rate at McFail's Cave shows a warmer and probably wetter period than at present from 7.0 to 7.6 ka. From 7.0 to 3.0 ka we see a steady progression towards the present cooler temperatures. The growth rates did not change markedly over this period, suggesting little change in precipitation or vegetational cover above the cave. From 2 to 0 ka there is little change in temperatures for this region. These findings regarding temperature are in general agreement with other paleoclimatic studies for this region. There is a brief warm spell centered on 2.5 ka that punctuates the cooler present temperatures. The highest $\delta^{18}\text{O}$ values were observed at the start of deposition of MF1, indicating the warmest temperatures, $\sim 5^\circ\text{C}$ warmer than present, though a shifting Jet Stream bringing isotopically heavier precipitation to the New York region would moderate this value somewhat. MF1 may however not record the time of peak temperatures of the Hypsithermal; a longer stable isotope profile of lake sediments from the region extending to 8.9 ka by (Anderson *et al.* 1997) also shows declining $\delta^{18}\text{O}$ (and therefore temperature) values, indicating that the maximum of the Hypsithermal may precede our inferred climatic optimum from MF1.

The $\delta^{13}\text{C}$ record showed some variability, with long-term changes in the density of the forest vegetation above the cave over this period. A spike of lower $\delta^{13}\text{C}$ values at ~ 7.5 ka shows an increase in productivity of the forest above the cave with the arrival of certain tree species (Prentice *et al.* 1991) which corresponds to the period of enhanced growth rate of stalagmite MF1. There was also a longer but less pronounced increase in forest density from 5.5 to 2.5 ka BP, suggesting increases in precipitation rates for the region.

ACKNOWLEDGEMENTS

This research has been made possible by NSERC grants to Schwarcz and Ford. Special thanks to Nicki Robinson for processing the U-series dates and Martin Knyf for assistance in the stable isotope analysis. We would also like to thank H.T. Mullins for his comments that helped improve this manuscript.

REFERENCES

- Anderson, W.T., Mullins, H.T., & Ito, E., 1997, Stable isotopic record from Seneca Lake, New York: Evidence for a cold paleoclimate following the Younger Dryas: *Geology*, v.25, p. 135-138.
- Baker, A., Smart, P.L., & Richards, A., 1993, Annual growth bandings in a cave stalagmite: *Nature*, v.272, p. 24-28.
- Baker, A., Genty, D., Dreybrodt, W., Barnes, W.L., Mockler, N.J., & Grapes, J., 1998, Testing theoretically predicted stalagmite growth rate with Recent annually laminated samples: implications for past stalagmite deposition: *Geochimica et Cosmochimica Acta*, v.62, p. 393-404.
- Baker, A., Genty, D., & Smart, P.L., 1998, High-resolution records of soil humification and paleoclimate change from variations in speleothem luminescence excitation and emission wavelengths: *Geology*, v.26, p. 903-906.
- Bar-Matthews, M., Wasserburg, G.J., Ayalon, A., & Kaufman, A., 1999, The Eastern Mediterranean paleoclimate as a reflection of regional events: Soreq Cave, Israel: *Earth and Planetary Science Letters*, v.166, p. 85-95.
- Brook, G.A., Rafter, M.A., Railsback, L.B., Sheen, S., & Lundberg, J., 1999, A high resolution proxy record of rainfall and ENSO since AD 1550 from layering in stalagmites from Anjohibe Cave, Madagascar: *Holocene*, v.9, p. 695-706.
- Broecker, W.S., Olsen, E.A., & Orr, P.C., 1960, Radiocarbon measurements and annual rings in cave formations: *Nature*, v.185, p. 93-94.
- Davis, M.B., Spear, R.W., & Shane, L.C.K., 1980, Holocene climate of New England: *Quaternary Research*, v.12, p. 240-250.
- Deines, P., 1980, The isotopic composition of reduced organic carbon, in Fontes, J.C. & Fritz, P., (eds.) *Handbook of Environmental Isotope Geochemistry. The Terrestrial Environment, Part A*: Elsevier, Amsterdam, p. 329-393.
- Dorale, J.A., Edwards, R.L., Ito, E., & Gonzalez, L.A., 1998, Climate and vegetation history of the midcontinent from 75 to 25 ka: A speleothem record from Crevice Cave, Missouri, USA: *Science*, v.282, p. 1871-1874.
- Dreybrodt, W., 1982, A possible mechanism for growth of calcite speleothems without participation of biogenic carbon dioxide: *Earth and Planetary Science Letters*, v.58, p. 293-299.
- Dwyer, T.R., Mullins, H.T., & Good, S.C., 1996, Paleoclimatic implications of Holocene lake-level fluctuations, Owasco Lake, New York: *Geology*, v.24, p. 51-522.
- Epstein, S., Lowenstam, H. Buchsbaum, R., & Urey, H.C., 1953, A revised carbonate-water isotopic temperature scale: *Geological Society of America Bulletin*, v.64, p. 1315-1326.
- Ford, D.C., & Williams, P.W. 1989: *Karst Geomorphology and Hydrology*: Unwin Hyman, London, p. 96.
- Forman, S.L., Oglesby, R., Markgraf, V., & Stafford, T., 1995, Paleoclimatic significance of late Quaternary eolian deposition on the Piedmont and High Plains, Central United States: *Global and Planetary Change*, v.11, p. 35-55.
- Foster, D.R., & Zebryk, T. M., 1993, Long-term vegetation dynamics and disturbance history of a Tsuga-dominated forest in New England: *Ecology*, v.74, p. 982-998.
- Frumkin, A., Ford, D.C., & Schwarcz, H.P., 1999, Continental oxygen isotopic record of the last 170,000 years in Jerusalem: *Quaternary Research*, v.51, p. 317-327.
- Frumkin, A., Carmi, I., Gopher, A., Ford, D.C., Schwarcz, H.P., & Tsuk, T., 1999, A Holocene millennial-scale climatic cycle from a speleothem in Nahal Qanah Cave, Israel: *The Holocene*, v.9, p. 677-682.
- Gascoyne, M., 1979, Pleistocene climates determined from stable isotope and geochronologic studies of speleothem: Unpublished Ph.D. thesis, McMaster University, p. 467.
- Gascoyne, M., 1992, Paleoclimatic determination from cave calcite deposits: *Quaternary Science Reviews*, v.11, p. 609-632.
- Genty, D., & Quinif, Y., 1996, Annually laminated sequences in the internal structure of some Belgian stalagmites-importance for paleoclimatology: *Journal of Sedimentological Research*, v.66, p. 275-288.
- Genty, D., Baker, A., & Barnes, W.L., 1997, Comparison entre les lamines luminescentes et les lamines visibles annuelles de stalagmites: *Compt. Rendus Acad. Sci.*

- Harmon, R.S., Schwarcz, H.P., & Ford, D.C., 1978, Stable isotope geochemistry of speleothems and cave waters from Flint Ridge-Mammoth Cave System, Kentucky: Implications for terrestrial climate change during the period 230,000 to 100,000 years B.P.: *Journal of Geology*, v.86, p. 373-384.
- Hendy, C.H., & Wilson, A.T., 1968, Palaeoclimatic data from speleothems: *Nature*, v.219, p. 48-51.
- Hennig, G.J., Grun, R., & Brunnacker, K., 1983, Speleothems, travertines and paleoclimates: *Quaternary Research*, v.20, p. 1-29.
- IAEA/WMO, 1998, Global Network for Isotopes in Precipitation. The GNIP Database. Release 3, October 1999.
- Jackson, S.T., & Whitehead, D.R., 1991, Holocene vegetation patterns in the Adirondack Mountains: *Ecology*, v.72, p. 641-653.
- Li, W., Lundberg, J., Dickin, A.P., Ford, D.C., Schwarcz, H.P., & Williams, D., 1989, High precision mass-spectrometric U-series dating of cave deposits and implications for paleoclimate studies: *Nature*, v.339, p. 534-536.
- Meese, D.A., Gow, A.J., Grootes, P., Mayewski, P.A., Ram, M., Stuiver, M., Taylor, K.C., Waddington, E.D., & Zielinski, G.A., 1994, The accumulation record from the GISP2 core as an indicator of climate change throughout the Holocene: *Science*, v.266, p. 1680-1682.
- Mullins, H.T., 1998, Holocene lake level and climate change inferred from marl stratigraphy of the Cayuga Lake Basin, New York: *Journal of Sedimentary Research*, v.68, p. 569-578.
- O'Neil, J.R., Adami, L.H., & Epstein, S., 1975, Revised value for the ^{18}O fractionation factor between H_2O and CO_2 at 25°C : *U.S.G.S. Journal of Research*, v.3, p. 623-624.
- Palmer, M.V., 1975, Ground-water flow patterns in limestone solution conduits: M.A. Thesis, State University of New York, Oneonta, NY, p. 28-40.
- Plummer, L.N., Parkhurst, D.C., & Wigley, T.M.L., 1979, Critical review of the kinetics of calcite dissolution and precipitation, in Jenne, E.A. (ed.) *Chemical Modeling in Aqueous Systems*: American Chemical Society, Washington, p. 537-573.
- Perrette, Y., Delannoy, J.J., Bolvein, H., Cordonnier, M., Destombes, J.L., Zhilinskaya, E.A., & Aboukais, A., 2000, Comparative study of a stalagmite sample by stratigraphy, laser induced fluorescence spectroscopy, EPR spectrometry and reflectance imaging: *Chemical Geology*, v.162, p. 221-243.
- Pielou, E.C., 1991, *After the Ice Age*: Chicago, Illinois, University of Chicago Press, p. 366.
- Prentice, C., Bartlein, P.J., & Webb III, T., 1991, Vegetation and climate change in eastern North America since the last glacial maximum: *Ecology*, v.72, p. 2038-2056.
- Railsback, L.B., Brook, G.A., Chen, J., Kalin, R., & Fleisher, C.J., 1994, Environmental controls on the petrology of a late Holocene speleothem from Botswana with annual layers of aragonite and calcite: *Journal of Sedimentary Research*, A64, p. 147-155.
- Roberts, M.S., Smart, P.L., & Baker, A., 1998, Annual trace element variations in a Holocene speleothem: *Earth and Planetary Letters*, v.154, p. 237-246.
- Rozanski, K., Araguas-Araguas, L., & Gonfiantini, R., 1993, Isotopic patterns in modern global precipitation: in *Climate Change in Continental Isotopic Records*: Geophysical Monograph 78. American Geophysical Union, Washington, p. 1-36.
- Ruddiman, W.F., 2001, *Earth's Climate: Past and Future*. Freeman and Co. New York.
- Schwarcz, H.P., 1986, Geochronology and isotopic geochemistry of speleothems: in Fontes, J.C., & Fritz, P., (eds.) *Handbook of environmental isotope geochemistry. The terrestrial environment*, B: Elsevier, Amsterdam, p. 271-303.
- Schwarcz, H.P., Harmon, R.S., Thompson, P., & Ford, D.C., 1976, Stable isotope studies of fluid inclusions and their paleoclimatic significance: *Geochimica et Cosmochimica Acta*, v.40, p. 657-665.
- Schwehr, K.A., 1998, Oxygen isotopic variations of soda straw cave deposits from the Yucatan Peninsula: A test of their use as a paleoprecipitation tool: Unpublished M.Sc. Thesis, University of Houston.
- Shopov, Y.Y., Ford, D.C., & Schwarcz, H.P., 1994, Luminescence microbanding in speleothems: High resolution chronology and paleoclimate: *Geology*, v.22, p. 407-410.
- Shopov, Y.Y., Ford, D.C., & Yonge, C.J., 1997, Speleothems as natural climatic stations with annual to daily resolution: *Proceedings of the 12th International Congress of Speleology*, La Chaux De Fonds, Switzerland, p. 105-106.
- Stuiver, M., Reimer, P.J., Bard, E., Beck, J.W., Burr, G.S., Hughen, K.A., Kromer, B., McCormac, G., van der Plicht, J., & Spurk, M., 1998, INT-CAL98 radiocarbon age calibration, 24,000-0 cal BP: *Radiocarbon* v. 40, p. 1041-1083
- van Beynen, P.E., 1998, Investigations into the Fluorescence of Calcitic Speleothems: Ph.D. Thesis, McMaster University, p. 103-137.
- White, W.B., 1997, Precise measurement of luminescence banding profiles in speleothems for paleoclimatic interpretation: *Proceedings of the 12th International Congress of Speleology*, La Chaux-de-Fonds, Switzerland, v.1, p. 89-92.
- Wigley, T.M.L., & Brown, M.C., 1976, The physics of caves: in Ford, T.D. & Cullingford, C.H.L. (eds.), *The Science of Speleology*: London, Academic Press, p. 329-358.
- Wigley, T.M.L., & Brown, M.C., 1978, Mass transfer and carbon isotope evolution in natural water systems: *Geochimica et Cosmochimica Acta*, v.42, p. 1117-1140.

***Limnodrilus hoffmeisteri* (ANNELIDA: OLIGOCHAETA: TUBIFICIDAE) IN POP'S CAVE, WISCONSIN, USA**

HOPE SWAYNE AND MICK DAY

Department of Geography, University of Wisconsin-Milwaukee, Milwaukee, Wisconsin 53201-0413 USA

hswayne@students.depaul.edu mickday@uwm.edu

MARK J. WETZEL¹

Center for Biodiversity, Illinois Natural History Survey, 172 Natural Resources Building, MC-652,

607 East Peabody Drive, Champaign, Illinois 61820-6917 USA. mjwetz@uiuc.edu

*Aquatic oligochaete worms identified as *Limnodrilus hoffmeisteri* were collected from rimstone pools in Pop's Cave, Richland County, Wisconsin, USA, in 1998. This represents the first record of aquatic oligochaetes from a cave in the state.*

Information on Wisconsin's caves and associated biological communities is limited at best. The karst in the southwestern part of the state – the Wisconsin Driftless Area – escaped the ravages of direct Pleistocene glaciation, but experienced the accompanying periglacial climate, which was followed by low mean annual temperatures in the Holocene. Cave air temperatures currently are about 10°C (Mueller & Day 1997). Moreover, the caves have been dismembered by valley incision, leaving them as ridgetop remnants without stream inputs (Day & Reeder 1989; Day *et al.* 1989). This combination of harsh Quaternary climatic conditions and restricted nutrient inputs has rendered Wisconsin's cave fauna impoverished. Barden (1980) described Wisconsin's caves as "...relatively lifeless", although they do provide habitats for various troglophiles, including insects, arachnids, millipedes, as well as rodents, bats, and some larger overwintering mammals. We know from other papers (e.g., Peck & Christiansen 1990; Webb *et al.* 1993; Culver *et al.* 2000; Buhlmann 2001; Culver 2001; Culver *et al.* 2003) that caves commonly support several other groups of troglophiles.

Despite their anonymity, the over 200 caves in southwestern Wisconsin are of scientific interest (Day 1986a,b,c). They are integrated into the regional karst hydrologic system (Reeder 1992; Reeder & Day 1993), and they provide evidence about former surface environments (Day 1988; Oh & Day 1990, 1991; Oh *et al.* 1991, 1993).

The presence of aquatic oligochaetes in Pop's Cave was first discovered by Hope and Jeff Swayne during a visit to the cave in June 1997 as part of a University of Wisconsin-Milwaukee Geography Department fieldwork course. The oligochaetes, estimated at 650 individuals in this population, were observed protruding from accumulated sediment in a series of small pools located about 60 m into the cave. These pools, each approximately 10 cm in depth, were impounded by rimstone (tufa) dams, and ranged in size from 20 to 50 cm in width and 0.5 to 2 m in length.

SITE DESCRIPTION

Pop's Cave, also known as Big Bear Cave, is located in Richland County, Wisconsin, 20 km west-northwest of the county seat of Richland Center. It is similar to other caves in southwestern Wisconsin, although it is consistently wetter than most, contains extensive breakdown, and lacks (in most sections) the ubiquitous, viscous red-brown silt and clay that characterizes other caves in the Wisconsin Driftless Area. Located on a ridge top south of and about 80 m above the valley of the West Branch of Mill Creek, the cave is developed in the Oneota member of the Lower Ordovician Prairie du Chien Group of carbonates (Paull & Paull 1977; Wisconsin Geological and Natural History Survey 1970) and is approximately 196 m in surveyed length, with main passages trending approximately north-south or northwest-southeast (Olmstead & Borman 1968). The elevation of the cave entrance is approximately 326 m a.m.s.l.; maximum depth of the cave is about 12 m.

The development of Pop's Cave was outlined by Olmstead and Borman (1968, 1980), who interpreted it as being of phreatic origin, with two main passage levels that were later connected through vadose collapse. Only the lowest, southwest section of the cave was infilled with sediment; elsewhere the breakdown deposits are being modified by calcite deposition, notably in the form of rimstone dams.

The cave is one of southwestern Wisconsin's most heavily visited; entries in the cave visitor registration book document at least 3000 visitors to the cave annually. Land use overlying and adjacent to the cave has three distinct components. The area above the northern third of the cave is wooded and is part of a Richland County scientific area. The land overlying the remainder of the cave was formerly in agricultural use, but has been enrolled in Wisconsin's Conservation Reserve Program for the past decade, and is now ungrazed grassland with encroaching trees and shrubs. By contrast, a 20-year old unof-

Please send correspondence to Mark J. Wetzel: mjwetz@uiuc.edu.

ficial garbage dump, littered with discarded appliances, abandoned vehicles, and decaying household refuse, is located immediately south of the cave. Organic contamination from this dump may provide nutrition to the oligochaetes via vadose seepage into the cave.

METHODS

Aquatic oligochaetes were collected from Pop's Cave by Hope and Jeff Swayne on 1 July 1998. Specimens and associated sediments were obtained from small rimstone pools using a kitchen ladle. Specimens were then isolated from the sediment by straining the water and sediment through a cotton cloth, and fixed in 10% formalin solution. After fixation for at least 24 hours, samples were rinsed in tap water, and transferred to 70% ethanol.

The specimens were permanently mounted on microscope slides and identified using compound microscopes equipped with phase and Nomarski differential interference contrast optics. Identifications followed Kathman and Brinkhurst (1998). Most of the specimens collected during this study are deposited in the INHS Annelida Collection in Champaign; several voucher specimens have been retained by the senior author.

RESULTS

Of the 112 oligochaete specimens collected, only 21 were sexually mature, all identified as *Limnodrilus hoffmeisteri* Claparède, 1862 (Oligochaeta: Tubificidae); no other tubificid species or representatives of other families of aquatic oligochaetes were collected. All immature specimens (n=91) were determined to be unidentifiable immature tubificids without capilliform chaetae.

DISCUSSION

Tubificids are a major component of the benthos in most freshwater environments, and are often abundant in polluted areas (Brinkhurst 1980; Brinkhurst & Cook 1974). They feed by ingesting sediment—anterior end buried in the sediment, posterior end protruding out of thin tubes of fine organic and inorganic material into the sediment-water interface. While feeding in a near-continuous, conveyor-like fashion, nutrition is extracted from the bacteria and organic matter associated with the sediments, and from their own fecal pellets that settle to the sediment-water interface (Brinkhurst 1974; Brinkhurst & Gelder 2001).

Limnodrilus hoffmeisteri, a cosmopolitan species occurring in a wide variety of surface water habitats, is perhaps the most ubiquitous and commonly collected freshwater tubificid worldwide. Both *L. hoffmeisteri* and *Tubifex tubifex* can be indicators of organic pollution and low levels of dissolved oxygen (Brinkhurst & Gelder 2001; Chapman & Brinkhurst 1984; Lauritsen *et al.* 1985), when they reach very high abun-

dance (Brinkhurst 1975; 1996). However, each of these species also has been associated with clean water benthic assemblages (Brinkhurst 1974).

Although this is the first published record of *L. hoffmeisteri* from a cave in Wisconsin, it has been reported from inland surface waters elsewhere in the state (Howmiller 1974, 1977; Howmiller & Loden 1976), in Illinois (Wetzel 1992), and is widespread throughout the Great Lakes (Spencer & Hudson 2003) and elsewhere in North America (Kathman & Brinkhurst 1998).

The presence of *Limnodrilus hoffmeisteri* and other oligochaete species in caves, springs, and groundwater habitats elsewhere in North America recently was reviewed in Wetzel & Taylor (2001), although only a few papers included species-level identifications of aquatic annelids among the often-extensive lists of reported taxa. In their limited surveys of eight caves in Illinois and Missouri, all associated with loess-covered karst terranes developed in Ordovician and Mississippian age bedrock (Panno *et al.* 1999), Wetzel and Taylor (2001) reported 15 taxa representing nine genera in five families. The abundance of new records reported by Wetzel and Taylor (2001) emphasizes the paucity of available information on aquatic Oligochaeta in North American caves; one and 10 species they collected were new records for the states of Illinois and Missouri, and several had never been reported from caves prior to their study.

We believe that tubificids and other aquatic oligochaetes are likely present, at least temporarily, in caves and other subterranean habitats elsewhere in the state into which surface and groundwater flows and accumulates, and where there are discrete connections between surface and underground streams.

Collecting techniques specifically designed for aquatic oligochaetes and other small invertebrates, in consultation with biologists who have taxonomic expertise with these groups, undoubtedly will result in the documentation of many new records for taxa from caves and associated groundwater habitats.

Culver *et al.* (2000) noted that under-representation of groups such as the aquatic oligochaetes in published accounts might alter our understanding of the taxonomic pattern of cave biodiversity in the United States. We therefore encourage use of appropriate collecting techniques for – and species-level identifications of – aquatic oligochaetes and other annelids in ecological studies of cave environments because they may comprise a significant and prevalent component of aquatic cave communities. The results of our preliminary research in Pop's Cave support continued study of Wisconsin's cave fauna – to determine if other oligochaete species are present in the caves, and to assess the status, distribution, and diversity of all aquatic invertebrates associated with or restricted to cave habitats.

The presence of *L. hoffmeisteri* in Pop's Cave suggests that the local cave and karst environment may reflect organic enrichment associated with fecal contamination such as that observed by Taylor *et al.* (2000) in their analyses of bacterial

fauna and water, sediment, and amphipod tissue chemistry of caves in the karst region of southwestern Illinois. Patterns of contamination arising from local agricultural activities deepen this concern (Day & Reeder 1989; Reeder 1992; Reeder & Day 1993), as does the widespread detection of regional groundwater contamination (Kammerer 1981).

ACKNOWLEDGMENTS

Funding for this project was provided in part by the University of Wisconsin-Milwaukee, Wisconsin Department of Natural Resources (undergraduate research project for H. Swayne), and the Illinois Natural History Survey Center for Biodiversity. We thank J. Swayne for extensive field assistance, and S.J. Taylor for providing background information. Preliminary identifications of some of the oligochaetes were verified by M.H. Winnell. We thank D.W. Webb, C.P. Weibel, D.C. Ashley, and two anonymous reviewers for assistance with this manuscript.

REFERENCES

- Barden, M., 1980, Biology of Wisconsin caves, in Alexander, E.C., (ed.), An Introduction to Caves of Minnesota, Iowa, and Wisconsin: NSS Convention Guidebook, no. 21, p. 108.
- Brinkhurst, R.O., 1974, Factors mediating interspecific aggregation of tubificid oligochaetes: Journal of the Fisheries Research Board of Canada, v. 31, p. 460-462.
- Brinkhurst, R.O., 1975, Oligochaeta, in Parrish, F.K., (ed.), Keys to the Water Quality Indicative Organisms of the Southeastern United States: Cincinnati, Ohio, U.S. Environmental Protection Agency, Office of Research and Development, Environmental Monitoring and Support Laboratory, p. 69-85.
- Brinkhurst, R.O., 1980, Pollution biology: the North American experience, in Brinkhurst, R.O. & Cook, D.G., (eds.), Aquatic Oligochaete Biology: New York, Plenum Press, p. 471-475.
- Brinkhurst, R.O., 1996, On the role of tubificid oligochaetes in relation to fish disease with special reference to the Myxozoa: Annual Review of Fish Diseases, v. 6, p. 29-40.
- Brinkhurst, R.O. & Cook, D.G., 1974, Aquatic earthworms (Annelida: Oligochaeta), in Hart, C.W., Jr. & Fuller, S.L.H., (eds.), Pollution Ecology of Freshwater Invertebrates: New York, Academic Press, p. 143-156.
- Brinkhurst, R.O. & Gelder, S.R., 2001, Annelida: Oligochaeta, including Branchiobdellidae, in Thorp, J.H. & Covich, A.P., (eds.), Ecology and Classification of North American Freshwater Invertebrates, Second Edition: San Diego, CA, Academic Press, p. 431-463.
- Buhlmann, K.A., 2001, A biological inventory of eight caves in northwestern Georgia with conservation implications: Journal of Cave and Karst Studies, v. 63, no. 3, p. 91-98.
- Chapman, P.M. & Brinkhurst, R.O., 1984, Lethal and sublethal tolerances of aquatic oligochaetes with reference to their use as a biotic index of pollution: Hydrobiologia, v. 115, p. 139-144.
- Culver, D.C., 2001, Subterranean ecosystems, in Levin, S.A. (ed.), Encyclopedia of Biodiversity, v. 5: Academic Press, San Diego, p. 527-540.
- Culver, D.C., Christman, M.C., Elliott, W.R., Hobbs, H.H., III, & Reddell, J.R., 2003, The North American obligate cave fauna: regional patterns: Biodiversity and Conservation, v. 12, p. 441-468.
- Culver, D.C., Master, L.L., Christman, M.C. & Hobbs, H.H., III, 2000, Obligate cave fauna of the 48 contiguous United States: Conservation Biology, v. 14, no. 2, p. 386-401.
- Day, M.J., 1986a, Cave studies in southwestern Wisconsin: implications and importance: The Wisconsin Speleologist, v. 19, no. 3, p. 1-21.
- Day, M.J., 1986b, Caves in southwestern Wisconsin, USA: Proceedings 9th International Speleological Congress, v. 1, p. 155-157.
- Day, M.J., 1986c, Caves in the Driftless Area of southwestern Wisconsin: The Wisconsin Geographer, v. 2, p. 42-51.
- Day, M.J., 1988, The origin of cave sediments in southwestern Wisconsin. Geol., v.15, p. 8-9.
- Day, M.J. & Reeder, P.P., 1989, Sinkholes and land use in southwestern Wisconsin, in Beck, B.F., ed., Engineering and Environmental Impacts of Sinkholes and Karst: Rotterdam, A.A. Balkema, p. 107-113.
- Day, M. J., Reeder, P.P. & Oh, J., 1989, Dolostone karst in southwestern Wisconsin: The Wisconsin Geographer, v. 5, p. 29-40.
- Howmiller, R.P., 1974, Studies on aquatic Oligochaeta in inland waters of Wisconsin: Transactions of the Wisconsin Academy of Sciences Arts and Letters, v. 62, p. 337-356.
- Howmiller, R.P., 1977, On the abundance of Tubificidae (Annelida: Oligochaeta) in the profundal benthos of some Wisconsin lakes: American Midland Naturalist, v. 97, no. 1, p. 211-216.
- Howmiller, R. & Loden, M.S., 1976, Identification of Wisconsin Tubificidae and Naididae: Transactions of the Wisconsin Academy of Sciences Arts and Letters, v. 64, p. 185-197.
- Kammerer, P.A., 1981, Groundwater Quality Atlas of Wisconsin: Wisconsin Geological and Natural History Survey Information Circular, no. 39, p. 1-39.
- Kathman, R.D. & Brinkhurst, R.O., 1998, Guide to the freshwater oligochaetes of North America: College Grove, Tennessee, Aquatic Resources Center.
- Lauritsen, D.D., Mozley, S.C. & White, D.S., 1985, Distribution of oligochaetes in Lake Michigan and comments on their use as indices of pollution: Journal of Great Lakes Research, v. 11, p. 67-76.
- Mueller, R.J. & Day, M.J., 1997, Daily atmospheric variation within caves in southwestern Wisconsin: Proceedings 12th International Speleological Congress, v. 1, p. 215-217.
- Oh, J. & Day, M.J., 1990, Loess-derived karst soils and sediments in the southwestern Wisconsin Driftless Area: The Journal of Regional Development (Korea), v. 15, p. 29-43.
- Oh, J. & Day, M.J., 1991, Sediments of the Seneca Sinkhole in the southwestern Wisconsin karst: The Wisconsin Geographer, v. 7, p. 25-39.
- Oh, J., Day, M.J. & Gladfelter, B., 1993, Geomorphic environmental reconstruction of the Holocene sinkhole sediments in the Wisconsin Driftless Area: Proceedings, Korean Scientists' and Engineers' International Conference (Geoscience Section), p. 390-397.
- Oh, J., Day, M.J., Gladfelter, B., Huppert, G., Fredlund, G. & Kolb, M., 1991, Potential sources of the sinkhole sediments in the Wisconsin Driftless Area: The Kyung Hee Geographical Review, no. 19, p. 31-58.
- Olmstead, R. & Borman, R., 1968, Origin and development of Pop's Cave: The Wisconsin Speleologist, v. 7, no. 2, p. 57-66.
- Olmstead, R. & Borman, R., 1980, Cavern development in Wisconsin—Active breakdown cave: Pop's Cave, Richland County, in Alexander, E.C., (ed.), An Introduction to Caves of Minnesota, Iowa, and Wisconsin, NSS Convention Guidebook No. 21, p. 121-123.
- Panno, S.V., Weibel, C.P., Wicks, C.M. & Vandike, J.E., 1999, Geology, hydrology, and water quality of the karst regions of southwestern Illinois and southeastern Missouri: ISGS Guidebook 27, Champaign, Illinois State Geological Survey.
- Paull, R.K. & Paull, R.A., 1977, Geology of Wisconsin and Upper Michigan: Dubuque, Iowa, Kendall/Hunt.
- Peck, S.B. & Christiansen, K., 1990, Evolution and zoogeography of the invertebrate cave faunas of the Driftless Area of the Upper Mississippi River Valley of Iowa, Minnesota, Wisconsin, and Illinois, U.S.A: Canadian Journal of Zoology, v. 68, p. 73-88.
- Reeder, P.P., 1992, Groundwater Contaminant Pathways in a Fractured Dolostone-Clastic Aquifer: Richland County, Wisconsin: University of Wisconsin-Milwaukee, PhD Dissertation, p. 1-463.
- Reeder, P.P. & Day, M.J., 1993, Seasonality of chloride and nitrate contamination in the southwestern Wisconsin karst, in Beck, B.F., (ed.), Applied Karst Geology: Rotterdam, Germany, A.A. Balkema, p. 53-61.
- Spencer, D.R. & Hudson, P.L., 2003, The Oligochaeta (Annelida, Clitellata) of the St. Lawrence Great Lakes region: an update: Journal of Great Lakes Research, v. 29, no. 1, p. 89-104.

- Taylor, S.J., Webb, D.W. & Panno, S.V., 2000, Spatial and temporal analyses of the bacterial fauna and water, sediment, and amphipod tissue chemistry within the range of *Gammarus acherondytes*: Illinois Natural History Survey Center for Biodiversity Technical Report 2000, no. 18, p. 1-115.
- Webb, D.W., Taylor, S.J. & Krejca, J.K., 1993, The biological resources of Illinois' caves and other subterranean environments: Illinois Natural History Survey Center for Biodiversity Technical Report 1993, no. 8, p. 1-168.
- Wetzel, M.J., 1992, Aquatic Annelida of Illinois: Introduction and checklist of species: Transactions of the Illinois State Academy of Science, v. 85, nos. 1 & 2, p. 87-101.
- Wetzel, M.J. & Taylor, S.J., 2001, First records of freshwater oligochaetes (Annelida, Clitellata) from caves in Illinois and Missouri, USA: Journal of Cave and Karst Studies, v. 63, no. 3, p. 99-104.
- Wisconsin Geological and Natural History Survey, 1970, Field Trip Guidebook for Cambrian-Ordovician Geology of Western Wisconsin: Wisconsin Geological and Natural History Survey Information Circular, no. 11, p. 1-131.

CAVE CONSERVANCY FOUNDATION GRADUATE AND UNDERGRADUATE FELLOWSHIP AWARDS

The Cave Conservancy Foundation is planning to award an Undergraduate Fellowship in Karst Studies for \$5000, an M.S. Graduate Fellowship in Karst Studies for \$5000, and a Ph.D. Graduate Fellowship in Karst Studies for \$15,000 in 2004. Any study of caves and karst in any field, including but not limited to archeology, biology, engineering, geography, geology, and social sciences, will be considered. The research can involve any cave and karst areas, including those outside the United States. Applicants must be full-time graduate or undergraduate students at a U.S. college or university.

Applicants for the undergraduate fellowship must include a letter of intent, a proposal of the research not to exceed 5000 words, a letter of support from an undergraduate advisor, and undergraduate transcripts. Mail applications before June 1, 2004 to Cave Conservancy Foundation, Attn: Undergraduate Fellowship Program, 13131 Overhill Lake Lane, Glen Allen, VA 23059. The award will be announced by July 1, 2004. For more information contact Dr. Horton H. Hobbs III, at Department of Biology, Wittenberg University, P.O. Box 720, Springfield OH 45501-0720, via e-mail at hhobbs@wittenberg.edu.

Applicants for the graduate fellowships (M.S. and Ph.D.) must include a letter of intent, a curriculum vita, a thesis proposal, graduate transcripts, and two letters of recommendation, one being from the thesis advisor. Mail applications before June 1, 2004 to Cave Conservancy Foundation, Attn: Graduate Fellowship Program, 13131 Overhill Lake Lane, Glen Allen, VA 23059. The awards will be announced by July 1, 2004. For more information contact Dr. David C. Culver, at Department of Biology, American University, 4400 Massachusetts Ave. NW, Washington, DC 20016-8007, via e-mail at dculver@american.edu.

ANNOUNCEMENT & CALL FOR ABSTRACTS: 2004 NATIONAL MEETING OF THE GEOLOGICAL SOCIETY OF AMERICA (NOVEMBER 7-10) FOR CAVE AND KARST SESSIONS

PERSPECTIVES IN KARST GEOMICROBIOLOGY AND REDOX GEOCHEMISTRY-TOPICAL SESSION #28

Questions may be addressed to Annette Summers Engel, University of Texas at Austin (aengel@mail.utexas.edu); Diana Northup, University of New Mexico (dnorthup@unm.edu); Toby Dogwiler, Winona State University (tdogwiler@winona.edu).

In the ten years since the Karst Waters Institute-sponsored conference, "Breakthroughs in karst geomicrobiology & redox geochemistry," there has been considerable progress in understanding microbial systems, geochemical processes, and the

interactions between them in cave and karst settings. We welcome contributions that highlight these major achievements and latest advances, and we encourage interdisciplinary participation from related hydrogeologic and biogeochemical settings.

FROM SUBTERRANEAN CRAWLWAYS TO SCIENTIFIC HALLWAYS: RESEARCH ON OUR PUBLIC CAVE AND KARST LANDS-TOPICAL SESSION #29

Questions may be addressed to Penelope J. Boston, National Cave and Karst Research Institute-New Mexico Institute of Mining and Technology (pboston@nmt.edu); Louise D. Hose, National Cave and Karst Research Institute-National Park Service (Lhose@cemrc.org)

Public lands provide unique natural laboratories and have facilitated important advancements in our understanding of cave and karst systems. This session focuses on both fundamental and significant discoveries to applied research in publicly managed karst terranes worldwide. Submissions of papers discussing or representing "Science in the service of public land management" and "Public lands in the service of science" are equally encouraged.

NEW AND MULTIDISCIPLINARY APPROACHES TO DATING CAVE DEPOSITS-TOPICAL SESSION #30

Questions may be addressed to Donald McFarlane (dmcfarla@jsd.claremont.edu) or Joyce Lundberg (joyce_lundberg@carleton.ca)

Resolving the ages of autochthonous and allochthonous deposits in caves is pivotal to a wide spectrum of research including archaeology, paleontology, paleoclimatology, and geomorphology. Although enormous advances have been made over the past 40 years, many challenges remain. This session aims to bring together researchers at the forefront of relevant technological and methodological advances, and those who are experimenting with, or successfully integrating multiple and/or innovative techniques to resolve long and complex speleological records.

There will be both ORAL and POSTER sessions for all these sessions.

HOW TO SUBMIT AN ABSTRACT:

The deadline for electronic abstract submission is July 13, 2004. The submission forms are available April 1-July 13, through the GSA's web site (<http://www.geosociety.org/meetings/2004/>). GSA requires that a speaker present only one abstract. If an author submits more than one volunteered abstract with the same person as speaker, all abstracts listing that speaker may be rejected. The abstracts are maintained and archived on the GSA's website.